

# Conduction velocities and nerve fibre diameters of touch, pain, urinary bladder and anal canal afferents and $\alpha$ and $\gamma$ -motoneurons in human dorsal sacral roots

Giselher Schalow<sup>1</sup>

## Abstract

1. Single action potentials were recorded extracellularly at 2 sites from human sacral dorsal nerve roots, and their conduction time measured. Conduction velocity frequency distribution histograms were constructed from afferent and efferent nerve fibres. Conduction velocity distribution peaks could be identified from afferents of mechanoreceptors of the skin, the bladder, the anal canal, of stretch and flow receptors of the urinary bladder, from spindle afferents and from the 3  $\alpha$  (extrafusal) and 3  $\gamma$ -motoneuron (intrafusal) classes.

The electrophysiologically measured roots were removed and morphometrically analysed. Nerve fibre diameter frequency distribution histograms were constructed with respect to 3 myelin sheath thickness ranges. Nerve fibre diameter distribution peaks could partly be correlated to the corresponding conduction velocity distribution peaks.

2. Identified nerve fibre classes, characterized by their group peak values of conduction velocity and fibre diameter were at about 36°C (age 30 years): Spindle afferents: SP1 (60 msec<sup>-1</sup>/13.2  $\mu$ m) SP2 (50/12.0?); touch afferents: TO (49 msec<sup>-1</sup>/13.0  $\mu$ m), T1 (44/11.2), T2 (39/10.1), T3 (31/9.1), T4 (20/8.3); pain afferents: P (13 msec<sup>-1</sup>?); mucosa touch afferents from bladder and anal canal: M (12.5 msec<sup>-1</sup>?); bladder afferents from stretch receptors measuring probably mural tension: S1 (42.5 msec<sup>-1</sup>?), ST (38/?) and from flow receptors: S2 (12.5/?);  $\alpha$ -motoneurons:  $\alpha_1$  (60 msec<sup>-1</sup>/13.1  $\mu$ m) [FF],  $\alpha_{11}$  (?/12.0) [F(int)],  $\alpha_2$  (50/10.2) [FR],  $\alpha_3$  (37/8.3) [S];  $\gamma$ -motoneurons:  $\gamma_\beta$  (27 msec<sup>-1</sup>/7.2  $\mu$ m),  $\gamma_1$  (20/6.7),  $\gamma_2$  (15/6.2).

3. Because of the strong temperature dependence of the conduction velocities a calibration of the structure of the velocities, which was almost independent of temperature, is defined by the condition that the  $\alpha_2$ -motoneurons have the same peak conduction velocity then the secondary spindle afferents (SP2); the T1 touch afferents have about 10% lower velocity values.

4. Touch afferents and  $\alpha$ -motoneurons had a different velocity-diameter relation, which indicated differences in the myelin sheath thickness and/or membrane properties. The conduction velocities of the touch afferents were more temperature-dependent than those of the  $\alpha$ -motoneurons. Within the classes of touch afferents and  $\alpha$ -motoneurons the temperature dependence increased towards smaller class peak values.

5. Through the use of action potential wave form comparisons it was possible to identify action potentials from single nerve fibres in each class of touch afferents (T0 to T4). Activity patterns of single touch units could partly be analysed. From delays and occurrence patterns of action potentials, stimulated by touch, it was found that the delay in T1 units which were not focally stimulated could be double as long as the delay in focally stimulated units for conduction distances of 550 mm. T1 units were probably most responsive to changes in the velocity of skin displacement. T3 and T4 units were more

<sup>1</sup> From the Ernst-Moritz-Arndt University Greifswald (Neurosurgery, Anesthesiology) and the Free University Berlin, Klinikum Steglitz (Neuropathology), Germany.

sensitive to light touch and/or had higher receptor densities than T1 and T2 units. T1 and T2 units probably adapted faster than T3, T4 and P units. The T0, T1, T2, T3 and T4 cutaneous mechanoreceptive afferents probably correspond to hair follicle, PC, RA, SAI, and SAII units respectively.

6. The action potential activity of the bladder afferents S1 and ST increased roughly proportionally with the filling of the bladder up to 750 ml. S1 and ST receptors probably measured mural tension. Flow receptors (S2) responded to fluid movements and the filling of the bladder, if this was higher than 600 ml (pressure).

7. The wall of the urethra contained mainly mechanoreceptors from mucosal M afferents. The wall of the anal canal contained mechanoreceptors from mucosal M afferents and, additionally, from the skin afferents T1, T2, T3 and T4. It is suggested that the different thresholds of the skin mechanoreceptors are used to distinguish flatus from fluid and feces in the anal canal.

8. Among nerve fibres with a diameter larger than  $5.5\ \mu\text{m}$  a dorsal S3 root contained very approximately 3% efferents, an S4 18% and an S5 root 20 to 30%.

9. It is discussed how the method of calculating peak conduction velocities and peak diameters of different nerve fibre classes can be used in experimental diabetes to recognize functional myelin sheath alterations before the morphological ones. A new diagnostic tool for neuropathies is suggested: By first recording extracellular action potentials from a nervus suralis fascicle before removing it from the patient for morphometry, it may also be possible to obtain conduction velocities of afferent nerve fibres and additionally of efferent nerve fibres, if they exist in the nervus suralis.

The anterior sacral nerve root stimulation for bladder control in paraplegia is discussed with respect to the existence of dorsal root efferents and ventral root afferents.

*Key-words:* Human — Nerve fibre classes — Group conduction velocity — Group diameter — Skin afferents — Anal canal afferents — Bladder afferents — Efferents.

## 1. Introduction

The motivation for this research is to develop treatment for spinal cord lesions. A reconnection of the human nervous system to restorate functions, (see clinical implications of the second paper (41)), can only be performed on rational grounds, if the functions of the human nervous system are known and can be varified anatomically and partly functionally during an operation.

In a series of 3 papers it will be shown that the extracellular recording of action potentials (Ap's) from the undamaged nervous system in connection with morphometry, can partly fulfil the task of clarifying the necessary function of the human nervous system and partly verify these functions in an operation in the form of diagnosis. In the first paper, it is mainly the method which is developed in order to identify

afferent and efferent nerve fibre classes in nerve roots. Activity patterns of afferents following natural stimulation supply information about receptor properties. The second paper reports upon activity patterns of motoneuron firing following physiological stimulations analysed in the first paper. The new observation, that motoneurons fire repeatedly with impulse trains (oscillatory firing mode) when high activity levels are needed, is analysed. One detailed measurement of urinary bladder filling is described. In the third paper activity changes of  $\alpha_2$ ,  $\alpha_3$  and  $\gamma$ -motoneurons in the occasional spike mode and the oscillatory firing mode are shown in response to skin, bladder and anal canal stimulations. Activity changes of secondary spindle afferents are given in response to  $\gamma$ -motoneuron activity changes. The clinical implications will deal with neuropathies in the first paper, treatment of spinal cord lesions in

the second paper and possibilities of disorders in the third paper.

In this first paper peak conduction velocities of myelinated afferent and efferent nerve fibre classes of known function will partly be correlated to their peak fibre diameters of measured distributions. Nerve fibres will be classified by paired values of group conduction velocity and group nerve fibre diameter instead of using the A, B and C system of Erlanger and Gasser (19) or the I to IV group system of Lloyd (33) for classification. It turns out that the relation between conduction velocity and nerve fibre diameter of a factor of 6 (25) is not a good description of human nerve fibre properties. Since there is no unique conversion factor between conduction velocity and nerve fibre diameter in animals (2, 7, 10, 21, 23, 50) and human (40), classes of nerve fibres are characterized by the group conduction velocity, the group nerve fibre diameter and its function.

In an earlier paper (40) 3 classes of  $\alpha$ -motoneurons and 3 classes of touch afferents were identified. These further, more detailed measurements support those data; small corrections have to be made to the  $\alpha_1$ -motoneurons and to the touch 2 and touch 3 afferents. The exactness of conduction velocity and nerve fibre diameter values given in this paper, again runs the risk of further corrections. But it is better to have precise data, which give detailed information and can be tested critically instead of having large ranges of values which cancel out properties.

## 2. Clinical material and method

Measurements were collected from 2 human cadavers (Cad), 5 brain dead human cadavers (Hirntote = HT's) and 1 patient (intraoperative diagnosis, Neuroleptanalgesia). There was no known neurological disease. It was attempted to keep the blood pressure up by administration of Dopamin (4  $\mu$ g/kg per min) according to those standards used in kidney removals. Elevated brain pressure, subarachnoidal bleeding, disturbance of coagulation and consumptive coagulopathy complicated the

trials. Only HT's, which could not be used for kidney explantation (infection, hypertension...), were used for the measurements.

### 2.1. Ethics

The measurements were done in accordance with the Declaration of Helsinki, and were to reconstruct urinary tract function as in kidney removals. The measurements on human cadavers, including HT's, for developing an operational technique in paraplegia, have been approved by the ethical committee of the GDR, where the measurements were performed. In West Germany (~60 000 000 inhabitants) there are about 1000 new paraplegics per annum. About 100 commit suicide because of the "no hope" situation. Others die because of chronic ascending bladder and kidney infections and the rest live with a low quality of life.

### 2.2. Electrophysiology

Action potentials (Ap's) were recorded extracellularly from nerve roots with 2 platinum wire electrode pairs (electrode pair distance = 8 mm; electrode distance in each pair = 4 mm) at 2 sites, preamplified ( $\times 1000$ ), filtered (RC-filter, passing frequency range 100 Hz-10 kHz) and displayed on a digital storage oscilloscope (Vuko Vks 22-16), and also stored using a PCM-processor (Digital Audio Processor PCM-501 ES) and a video recorder (JVC-Kassettenrecorder, Modell Nr. Hr-D250 EG) (40). A sharp 50 Hz filter was sometimes used between the preamplifier and the scope or when recalling from the tape between the processor and the scope. Mostly, the time at the beginning of a touch with a metal ball ( $\varnothing = 5$  mm) or of pricking with a pin was marked with an upward pulse and the end of a touch or pin-pricking with a downward pulse on trace "a". These pulses were generated by a markation pulse generator connected to the digital scope, which was switched on and off with a touch sensor working on the basis of resistance changes. To reduce the contact resis-

tance between touch ball and skin contact gel was used for the skin. Also, the pulling and releasing of the anal and bladder catheters were mostly marked with a pull-switch connected to the catheters and working in connection with the same markation pulse generator. Conduction velocities of single fibres were calculated from the conduction distance (electrode pair distance) and their conduction times, the time needed for an Ap to cover the conduction distance (time difference between the traces "a" and "b" for a certain Ap). Trace "a" was the recording from the proximal electrode pair and trace "b" from the distal pair. Conduction velocity frequency distribution histograms were constructed. Histogram classes were  $\leq$  and  $<$ . To obtain a sufficient number of occurring conduction velocities, several histograms of several time intervals of 400 msec were lamped together. If all occurring velocities were used (open plus hatched part of histograms), the overall activity was obtained. For getting information about the number of active fibres, each conduction velocity value was used only once (hatched part of the histograms); for an explanation of the hatched and open plus hatched histograms see reference 40; page 36. This measure of the number of active fibres is rather arbitrary since it depends on the overall activity, the accuracy of the measurements and the repeatability of the true conduction velocity, and gives only approximate information about active nerve fibre numbers. However, it is quite good for comparing the activated number of fibres of comparable histograms. A better measure of active nerve fibre numbers is the identification of single fibres by wave form considerations on the proximal (a) and distal (b) traces. The number of existing fibres, both active and inactive, were obtained from nerve fibre diameter frequency distribution histograms if distribution peaks (groups) could be identified. The error of a measured conduction velocity depended on the accuracy of the measurement, on the digitalisation (how many digital points per Ap) and on the noise and artifact level. With 8192 digitalisation points per sweep (256 points in  $y$ -direction), the quality of digitalisation changed with the chosen time scale. Addi-

tionally, the Ap's from a single fibre were not always conducted with exactly the same velocity, as could be measured from repeatedly firing fibres.  $\alpha$ -designates extrafusal motoneurons and  $\gamma$ -intrafusal ones. No special care was taken in this first paper for the oscillatory firing mode of a few  $\alpha$ -motoneurons, since the conduction velocity distribution peaks of motoneurons were only used as a calibration marker. For further details of the recording method see references 40 and 61.

### 2.3. Morphometry

Root pieces of a few cm were removed from the HT's after recording and from cadavers (Cad), fixated for 2 to 4 hours in 4% glutaraldehyd in cacodylate buffer, afterwards fixated in 1% OsO<sub>4</sub> for 2 hours and dehydrated and embedded in Araldite according to standard techniques. Pictures of semi-thin sections, stained with thionin acridine-orange, were taken with the light microscope ( $\times 1000$ ). Nerve fibre diameters  $\varnothing = 1/2(\varnothing_1 + \varnothing_2)$  ( $\varnothing_1$  and  $\varnothing_2$  are the larger and smaller diameter of non-roundshaped fibres) and the mean myelin sheath thickness "d" were measured by hand. A shrinkage correction of 8% was taken into account. The measured nerve fibre diameters were divided up in 4 myelin sheath thickness ranges ( $d = 0.25-0.75 \mu\text{m}$ ,  $d = 0.8-1.25$ ,  $d = 1.3-1.75$ ,  $d = 1.8-2.3$ ;  $d$ -values were measured in steps of  $0.05 \mu\text{m}$  so that there are no gaps between the  $d$ -ranges), of which 3 were plotted in the figures 11 and 12. The histogram classes were  $\leq$  and  $<$ . Electron micrographs were only used for the control of the light microscope pictures. For further details see reference 40.

## 3. Results

### 3.1. Electrophysiology

#### 3.1.1. Touch afferents from the nearly hairless skin

Action potential (Ap) activity in response to touching sacral dermatomes is shown in fig-

## Touch-stimulated afferent activity

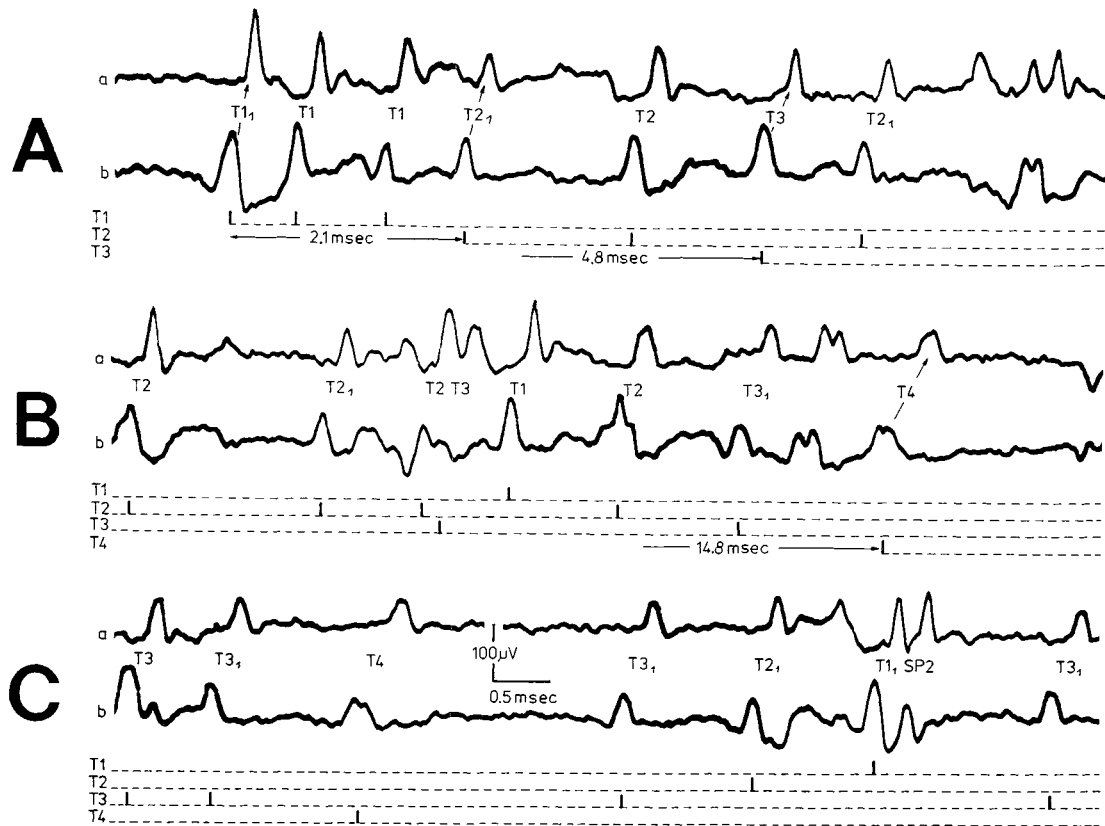


Fig. 1. — First part of touch stimulated activity from an S4 ventral root recording, HT3. A, B, C are successive sweep pieces. Touching area about 15-20 mm in diameter (touching with a finger). Extracellular action potentials (Ap's) are marked with the touch afferent groups (T1, T2, T3, T4) to which they belong according to the conduction velocity distribution histogram of figure 2. Subscripts mark Ap's from single fibres. Traces "a" and "b" in A, B, C are original registrations. The dashed line traces T1, T2, T3, T4 below trace "b" give the activity of separated touch groups schematically. Each upward deflection marks the occurrence of an Ap. Notice, the Ap's of group T2 arrive 2.1 msec later at the place of measurement than the Ap's from the T1 group. The Ap's from the T3 and T4 group arrive 4.8 and 14.8 msec later. SP2 marks the Ap from a secondary spindle afferent fibre.

ure 1 in a ventral S4 root recording. The corresponding conduction velocity distribution histogram was constructed (Fig. 2A). The 5 activity peaks in figure 2A were marked with T0, T1, T2, T3 and T4 and interpreted as 5 groups of touch afferents with certain conduction velocity distribution ranges. The extracellularly recorded Ap's of figure 1 were then marked with the group they belong to according to their conduction velocity values. The Ap's of a certain touch group could originate from 1 or several touch units. By recognizing very similar wave forms on the traces "a" and "b", a few Ap's were identified as originating

from the same fibre and were marked with an index. Not all wave form identifications were safe, but the approximate number of units in each class of figure 1 could be counted and amounted to 3 in T1, 3 in T2, 3 in T3 and 1 in T4. The sweep piece of figure 1 is therefore a recording of about 10 touch units. Ap's from the group T0 do not occur in this sweep piece. The Ap's with shorter conduction times (higher conduction velocities) have, on average, higher amplitudes.

In the lower part of figures 1A, B and C the arrival of the first Ap's from the fastest touch units of the T2, T3 and T4 groups are given in

relation to the arrival of the first Ap from the fastest unit of the T1 group. With these relative latencies and the group conduction velocities (peak values), it will be calculated how far the place of touching sacral dermatomes was away from the recording electrodes. Instead of solving algebraic equations, a few values were chosen and varified that a distance value of 550 mm fits best, as will be shown. Temperature-corrected conduction velocities were used from figure 13:  $v(T1) = 44$  m/sec;  $v(T2) = 39$ ;  $v(T3) = 31$ ;  $v(T4) = 20$ . The absolute latencies ( $v = \text{distance}/\text{latency}$ ) are: Latency(T1) = distance/ $v(T1) = 550 \text{ mm}/44 \text{ mm}(\text{msec}^{-1}) = 12.5 \text{ msec}$ ;  $l(T2)$

= 14.1;  $l(T3) = 17.7$ ;  $l(T4) = 27.5$ . The relative latencies are  $l_r(T2) = 14.1 - 12.5 = 1.6 \text{ msec}$ ;  $l_r(T3) = 5.2$  and  $l_r(T4) = 15$ . The calculated values of 5.2 and 15 msec of the T3 and T4 groups are in good agreement with the measured values of 4.8 and 14.8 msec of figure 1. Therefore the calculated distance between the recording and the stimulation place was roughly 550 mm. The measured distance between the proximal cauda equina and the place of touch (S4 dermatome on top of the gluteus maximus) was between about 500 and 600 mm. The measured value and the calculated value are compatible. Only the measured relative latency of the T2 unit of 2.1 msec is a bit

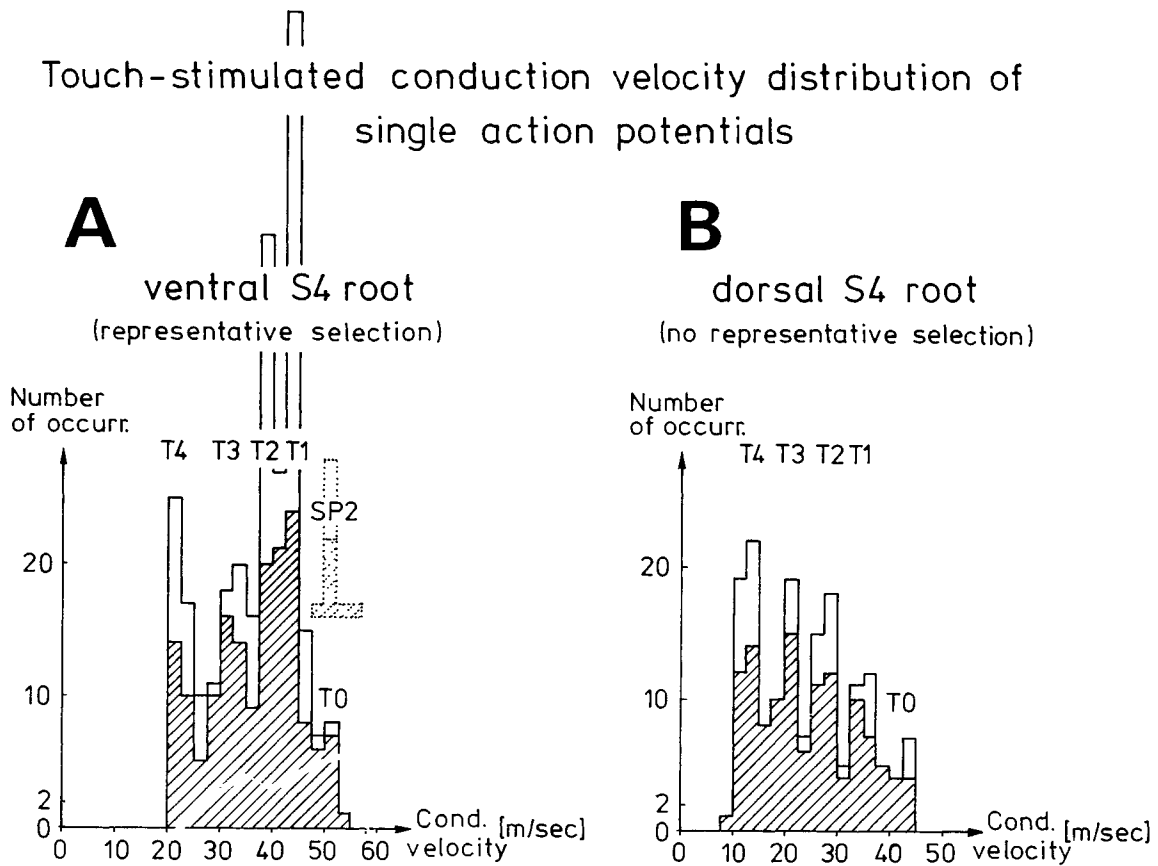


Fig. 2. — Conduction velocity frequency distribution histograms of touch stimulated afferents. Hatched part, each conduction velocity value taken only once; open plus hatched part, all values are taken. T0, T1, T2, T3, T4 = distribution peaks of touch-stimulated afferents.

A. Sum of 5 histograms, each of a single sweep, containing the whole activity in response to one touch with a finger. The sweep of figure 1 is included. The histogram shows a representative activity selection. Indicated spindle afferents (SP2) are mainly from activity before and after the touch activity. Ventral S4 root, HT3.

B. Sum of 3 histograms, each from a single touch with a metal ball of 5 mm diameter at about the same place. No representative selection since Ap's merged, especially from T1 and T2. Dorsal S4 root, HT6.

too long in comparison to the calculated value of 1.6. Other factors have to be taken into consideration. As will be shown in section 3.1.4 (Fig. 5), one of these factors is how focally a touch receptor is stimulated.

Figure 2A shows the conduction velocity distribution histogram for the touch afferents of an S4 ventral root. Since the activity was rather low (Fig. 1), the Ap's only sometimes merged. The number of measured conduction velocities is therefore representative for the activity. The T1 touch group contains the most Ap's and the T2 group the second highest amount for a touch of medium strength. In a histogram of an S4 dorsal root (Fig. 2B) 5 touch peaks can again be identified, but the T1 and the T2 peaks are much smaller. Since a dorsal root normally contains many more afferents than a ventral one, the activity mostly becomes so high that Ap's merge quite often and the corresponding conduction velocities are lost for the histogram. Since the number of merging Ap's is not proportional for the different groups (see Ap density distribution in Fig. 5) the histogram becomes non representative with respect to the size of the peaks. The peak conduction velocity values are not altered very much in comparison to the values from representative activity histograms. All touch peak values measured are summarized in table 1.

Since the histograms of figure 2 were constructed from measurements at different temperatures, the conduction velocity values of each group (peak values) are different for the 2 cases. One could try to correct temperature differences with a certain factor (13, 37). But since the temperature dependence of the conduction velocities is not the same for different groups of touch afferents (Fig. 15), a calibration will be introduced in the next section to partly overcome the temperature problem.

### 3.1.2. Calibration of afferent and efferent conduction velocities

Since in the lower sacral roots there are mostly a few afferents in the ventral (motor) roots (40) and a few efferents in the dorsal root (61, Table 1), the correlation between

easily identifiable afferent and efferent conduction velocity distribution peaks offers the possibility of calibrating conduction velocity distributions. Conduction velocity peaks can then be identified relatively by their position in relation to the calibrating peaks, which are measured simultaneously and absolute peak values can be obtained from a known conduction velocity value distribution (Fig. 13) at a useful temperature (36°C).

Now such a hierarchy of peak conduction velocities with its marker velocities will be built up. Figure 3 shows the afferent and efferent conduction velocity distributions from an L4 root filament to which  $\alpha$ -motoneuron (40) and touch afferent peaks (Fig. 2) from an S4 ventral root of the same HT (HT3) had been added. The nerve root temperature of these measurements was about 36°C. As can be seen from figure 3 (and Table 1) the conduction velocity values of the  $\alpha_1$  and  $\alpha_2$ -motoneurons are very

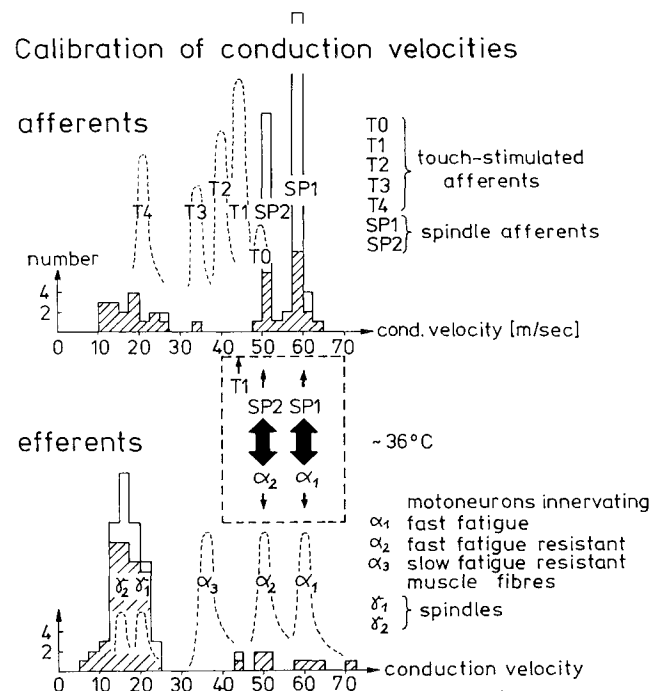


Fig. 3. --- Calibration of conduction velocities of afferent and efferent nerve fibres. Black double arrows mark similar conduction velocities of afferents and efferents. Note, the  $\alpha_2$ -motoneurons have about the same conduction velocity as the secondary spindle afferents (SP2), the T1 touch afferents conduct about 10% slower. L4 plus S4 roots, HT3. Root-temperature  $\sim 36^\circ\text{C}$ .

similar to the primary and secondary spindle afferents respectively (for identification see later) and are marked with black double arrows. The best calibration marker for the lower sacral nerve roots seem to be the correlation between the  $\alpha_2$ -motoneurons and the T1 touch afferents, since the  $\alpha_2$ -motoneurons show the largest  $\alpha$ -motoneuron peak in the lower sacral roots and are always present and the T1 touch afferents build up the largest peak among the other touch afferents and are easily stimulated, only the T1 peak conduction velocity is 10% lower than the  $\alpha_2$ -motoneuron peak conduction velocity. In most of the following given conduction velocity distributions, the simulta-

neously measured  $\alpha_2$ -motoneuron or T1 touch afferent peaks are also given for calibration.

Since many groups of afferents exist, they can have similar or same conduction velocity peak values. Nerve fibre diameter peaks or functional identification additionally are needed for the characterization of nerve fibre groups.

### 3.1.3. Fast pain (and touch) afferents of the skin

By sticking a pin in the lower sacral dermatomes, the conduction velocity frequency distribution of figure 4A was obtained. The upper part of figure 4A shows a new pain peak P in addition to the touch peaks. In the lower part of figure 4A there is the measured motoneuron

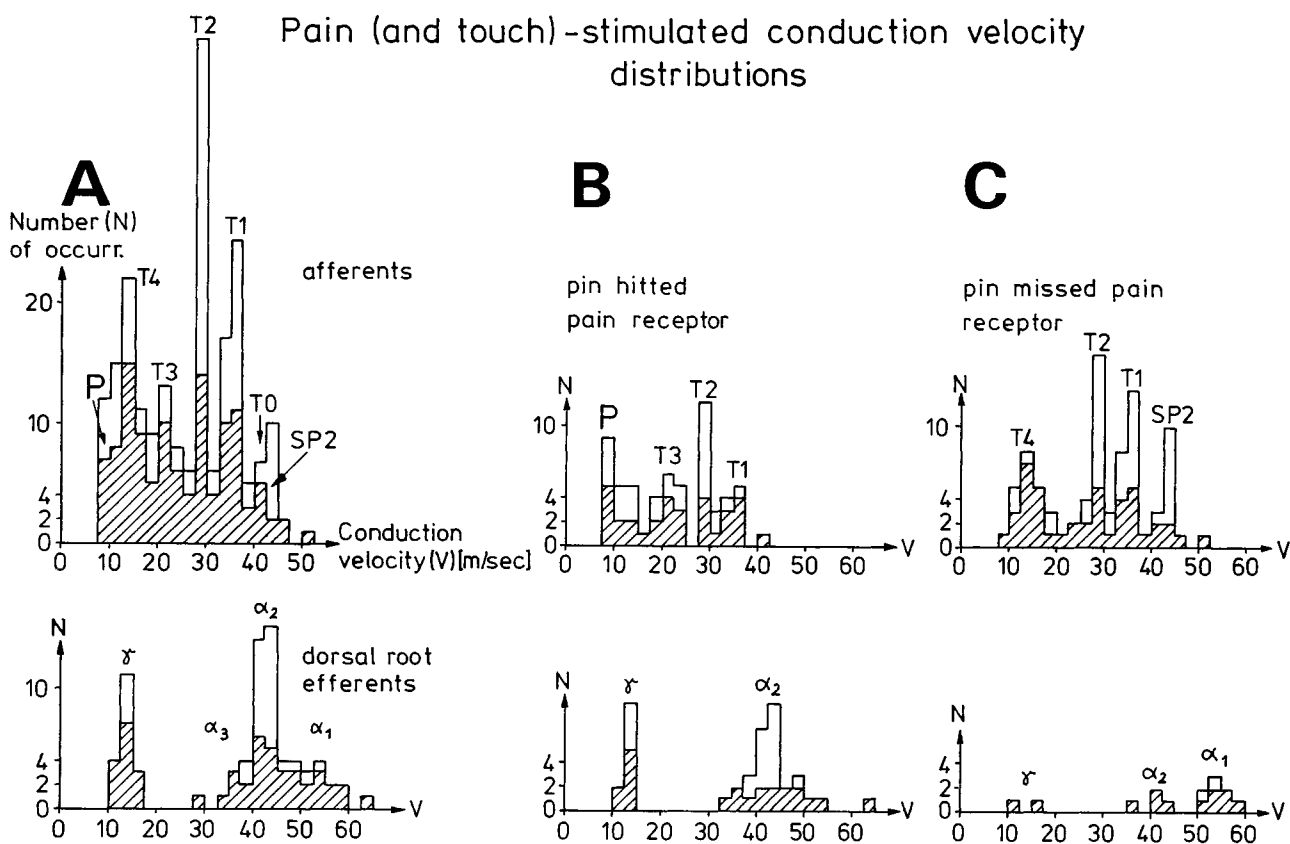


Fig. 4. — Conduction velocity distribution histograms of pain and touch-stimulated afferents of a dorsal S4 root (HT6) when pricking lower sacral dermatomes with a pin. Upper histograms from afferents, lower ones from simultaneously measured efferents.

A. Histogram as a sum of 3 histograms (2 of them in B and C) from 3 single pin-pricks at about the same place. P = pain peak, T0, T1, T2, T3, T4 = touch distribution peaks, SP2 = secondary spindle afferent peak,  $\alpha_1$ ,  $\alpha_2$ ,  $\alpha_3$ ,  $\gamma$  = motoneuron peaks.

B. Histogram of 1 sweep from a single pin-prick, pain receptor probably hit.

C. Histogram of 1 sweep, when the pin most likely missed the pain receptor.



distribution given for the calibration. To get more information about the stimulated pain afferents and simultaneously stimulated touch afferents, single sweep distributions of pin-prickings are shown in the figures 4B and C. It can be seen from figure 4B that this pin-pricking mainly stimulated pain and T1, T2 and T3 touch receptors since peaks from their afferents appeared in the histogram. The peaks of the  $\alpha_2$  and  $\gamma$ -motoneurons are large, indicating a  $\alpha_2$ - $\gamma$ -coactivation. Further details about the  $\alpha_2$ - $\gamma$ -coactivation will be given in the third paper. In figure 4C the histogram from another pin-pricking is shown where mainly the T1, T2 and T4 peaks are present, but not the pain peak. Motoneurons were only activated a little. Most likely the pin missed the pain receptors which gave rise to the pain peak.

Since it has only been possible, so far, to record activity from receptors which have afferents thicker than about  $5.5 \mu\text{m}$  (Figs. 11 and 13), one has no information about the stimulated activity of receptors with afferents thinner than  $5.5 \mu\text{m}$ . The pain activity recorded here is most likely from pain receptors whose afferents conduct fastest, which means, in that kind of interpretation, that one records here the fast pain or one component of the fast pain.

The hatched part of conduction velocity distribution histograms of single sweeps (Fig. 4B and C) gives some information about the number of stimulated afferent units. More exact information about the number of stimulated mechanoreceptors of the skin can be obtained by action potential wave form identifications. With the single fibre identification the activity patterns of single mechanoreceptor units can also be studied further in a population of units, as will be seen in the next section.

#### 3.1.4. *Some properties of mechanoreceptors of the skin*

In figure 5 the recorded activity is shown when sticking S5 or coxygeal dermatomes with a pin. The activity pattern shows a touching and a releasing part of activity as can be seen from the action potential (Ap) appearance of large amplitude (T1 and T2 units) and from the

schematic activity pattern of the T1 units in the lower part of figure 5A. All the 4 touch (T1 till T4) and 1 pain groups, recorded here, seem to have their own touching and releasing part, but, according to their latencies and conduction velocities, at different times. It can be seen from figure 5 that the touching activity part of the slower conducting T3 and T4 fibres with their smaller Ap amplitudes (Figs. 5A and C) started about in the middle of the T1 and T2 activity part and lay mainly between the touching and releasing parts of the T1 and T2 units. The releasing activity of the T3 and T4 fibres appeared after that of the T1 fibres. The activity of the pain fibres (here the slowest conducting fibres) appeared even later at the recording electrodes and stopped appearing after the end of the pin-pricking (recorded at the proximal cauda equina).

The very late pain after pin-pricking which one normally also feels is probably conducted by very thin myelinated or non-myelinated fibres and cannot be recorded here.

In the T1 touch group, 3 units could be identified by wave form considerations. It will now be analysed in more detail in figure 5, together with the activity pattern of these 3 units, why the touching part of activity normally had a higher and longer lasting activity than the releasing part and it will be attempted to clarify, why T1 units can have quite different delays, which cannot be explained by conduction velocity differences alone. In the lower part of figure 5A the activity pattern of each T1 unit is schematically redrawn. It can be seen that all 3 units had a different delay and that the releasing activity of the T1<sub>2</sub> unit nearly fell into the touch activity part of the T1<sub>1</sub> unit and that the T1<sub>3</sub> unit responded only with a touching part of 1 Ap. With the additional information that the T1<sub>1</sub> unit responded with 3 Ap's, the T1<sub>2</sub> unit with 2 and the T1<sub>3</sub> unit only with 1 Ap, these activity patterns are interpreted with the spatial distribution of the receptors of these 3 T1 units (Fig. 5A, insertion "2"). The T1<sub>1</sub> unit had its receptor nearest to the needle (Fig. 5A, insertion "2") and responded fastest and longest since the skin indentation first reached the T1<sub>1</sub>

## Touch (and pain) -stimulated afferent activity

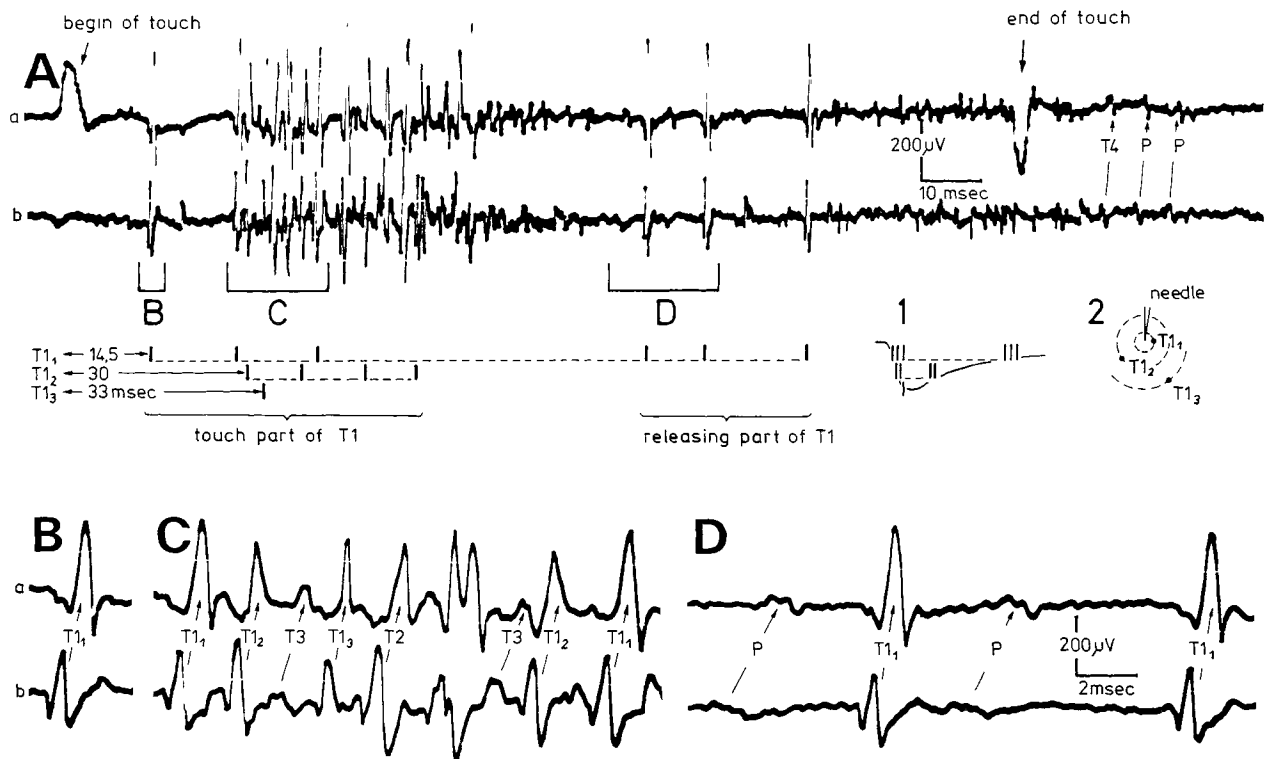


Fig. 5. — Touch and pain activity stimulated by pricking with a pin S5 or Co dermatomes and recording extracellularly from a dorsal coxygeal root (HT6). T1, T2, T3, T4, P = mark Ap's from touch and pain fibres. Subscripts 1, 2, 3 mark single fibres.

A. Whole sweep shown at a slow time base. Large upward artifact on trace "a" marks electronically the beginning of the touch. Large downward artifact on trace "a" marks the end of the skin touch. Note that 2 intervals of high activity of large Ap's occur, one after the beginning of the touch with 1 Ap in front, and a second before the end of the touch; potentials with small amplitude follow the potentials of large amplitude. Time intervals B, C and D are shown in a time-expanded form in figures B, C and D. Ap's from 3 T1 units are schematically shown by dashed lines and upward deflections in the lower part of A. Latencies are indicated. Insertion "1" shows schematically the activity pattern (dashed lines with deflections) in relation to the indentation of the skin. Insertion "2" shows schematically the spatial distribution of the corresponding T1 receptors. The dashed circles indicate the possible places of 1 receptor belonging to the T1<sub>1</sub>, T1<sub>2</sub>, T1<sub>3</sub> units.

B, C, D. Time expanded sweep pieces of A. Identified Ap's are indicated. Note that the Ap's from the T1<sub>1</sub> touch unit can be safely identified by the wave forms in B, C, D.

receptor, gave rise to the largest skin shift and turned away last (Fig. 5A, insertion "1"). The T1<sub>2</sub> receptor, being further away from the centre of skin touch, was reached later by the skin indentation, the skin shift was not so large and the skin turned back to the former position quicker. The Ap's in the T1<sub>2</sub> unit therefore appeared later, showed only 2 Ap's in the impulse train and the release activity part also

appeared earlier. The T1<sub>3</sub> receptor, lying furthest away from the centre of skin indentation, was reached last, with just a threshold skin indentation, and responded with 1 Ap.

From figure 5A it can be seen that the T1 units adapted rapidly. But the dependence on the time course of the skin indentation may be even stronger than the dependence on velocity. As can be seen from the lower part of figure 5A

the T<sub>1</sub> unit had the shortest latency, the T<sub>12</sub> unit the second shortest and the T<sub>13</sub> unit the longest latency. This was explained simply by the time the beginning of the skin indentation needed to propagate to the different T1 receptors, which means it was explained by the closeness, at which a receptor is stimulated. If one receptor is stimulated very closely and the other ones are not, than 1 Ap will be quite far in front of the other ones as in figure 5A due to the very short latency of the focally stimulated receptor. But if 2 receptors are stimulated only half-focally, than no Ap will lead clearly. The focality argument can explain the often-observed phenomenon that 1 Ap led ("B" in Fig. 5A). But it is difficult to understand why that leading was sometimes so strong or why the latencies in the T1 group were so different. The T<sub>12</sub> unit had a latency more than double as long as the T<sub>1</sub> unit, even though its conduction velocity was a bit faster (for shorter conduction time see Figs. 5B and C), whereas the T<sub>13</sub> unit had an unproportional, only slightly longer latency than the T<sub>12</sub> unit.

If one splits the latency into a first part — the time needed from the beginning of the touching of the skin till the occurrence of the Ap's in the receptor ( $l_1$ ), a second part — the time needed for the Ap to travel from the receptor to the place, where the unit fibre starts, which will be neglected here and does not exist if a unit has only one receptor, and a third part — the time needed for the Ap to travel from the beginning of the unit-afferent fibre to the measuring place ( $l_2$ ), than one can calculate the latencies  $l_1$  and  $l_2$  from the temperature corrected T1 group conduction velocity of 44 m/sec from figure 13, the distance of about 550 mm from the receptors to the recording place and the 3 overall latencies of the 3 T1 units, namely 14.5 msec (T<sub>1</sub>), 30 (T<sub>12</sub>) and 33 (T<sub>13</sub>) from figure 5A:  $l_2(\text{T1}_1, \text{T1}_2, \text{T1}_3) = 550 \text{ mm}/44 \text{ mm (msec}^{-1}) = 12.5 \text{ msec}$ ;  $l_1(\text{T1}_1) = l - l_2 = 14.5 - 12.5 = 2 \text{ msec}$ ,  $l_1(\text{T1}_2) = 30 - 12.5 = 17.5 \text{ msec}$  and  $l_1(\text{T1}_3) = 33 - 12.5 = 20.5 \text{ msec}$ . The difference of the  $l_1$  latencies between the T<sub>1</sub> and T<sub>12</sub> units is  $l_1(\text{T1}_2) - l_1(\text{T1}_1) = 17.5 - 2 = 15.5 \text{ msec}$  and the one between the T<sub>12</sub> and the T<sub>13</sub> unit is

3 msec (20.5 – 17.5). It does seem that not only spatial differences (Fig. 5A, insertion "2") can account for a  $l_1$  latency difference of a factor of 5. It is very likely that the T1 receptors also depend on the acceleration with which the skin around the receptor is shifted. The acceleration of skin shift will be highest at the most focally stimulated T<sub>1</sub> receptor. It is, therefore, concluded that the T1 receptors are also acceleration dependent receptors.

As can be seen from figure 5C, the first Ap from a T2 touch unit arrived later than those from the T3 unit. It could be that the T2 touch units have similar properties with respect to latencies than the T1 units. This would explain the relatively long latency of the T<sub>21</sub> unit in figure 1.

Properties of T1 and T2 units will now be further compared with the ones of the T3 and T4 units. A touch with a metal ball or a pin of medium strength, as analysed before in figure 5, stimulated the T1 to T4 touch units to generate a response with the beginning and with the end of the touch. The order of the activity appearance of the different groups is roughly given by the conduction velocity of each group, that means the activity parts of the T1 and T2 touch units are recorded before the activity parts of the T3 and T4 (Fig. 1). This order of the occurrence of Ap's from the different touch groups changed when a light or a very light touch was applied. In the case of a light touch, the T3 and T4 units occurred before the T1 and T2 units. For a very light touch, one T1 potential but a few T3 and T4 Ap's occurred. It is concluded that the T3 and T4 touch units are more sensitive to light touch and/or have a higher receptor density than the T1 and T2 touch units.

From 6 touch stimulations, like the one in figure 5A, the latencies, the length of the touch and the releasing activity parts were measured from the T1 and T2 units and from the T3, T4 and P units. The mean latencies of the T1 and T2 units (the first occurring Ap was taken as the measure) was 16 msec (2 latencies were left out because of enormous length due to a very light touch) and the mean latency of the T3, T4 and P units was 32 msec (see also Fig. 5C). This

latency length can be mainly understood with the differences in the conduction velocities. The duration of the touch and the releasing activity parts of the T1 and T2 units were 35 and 16 msec respectively, those of the T3, T4 and P units were 68 and 45 msec respectively. It is concluded that the T1 and T2 units adapt more rapidly than the T3, T4 and P units.

Little is known about the T0 units. Their Ap's appeared with the touch. They conducted fastest among the touch units, but their Ap's did not have the shortest latency.

### 3.1.5. Afferents from mechanoreceptors of the mucosa of the bladder

Due to later use for diagnosis, mechanoreceptors of the bladder mucosa were stimulated with a bladder catheter. In this way one stimulates the trigonum vesicae, the urethra, the ostium urethrae externus and maybe the pubic region.

Figure 6 shows conduction velocity distribution histograms, constructed from the recordings of the activity increase due to the pulling of the bladder catheter. By recording from an

## Conduction velocity distributions from bladder catheter stimulation

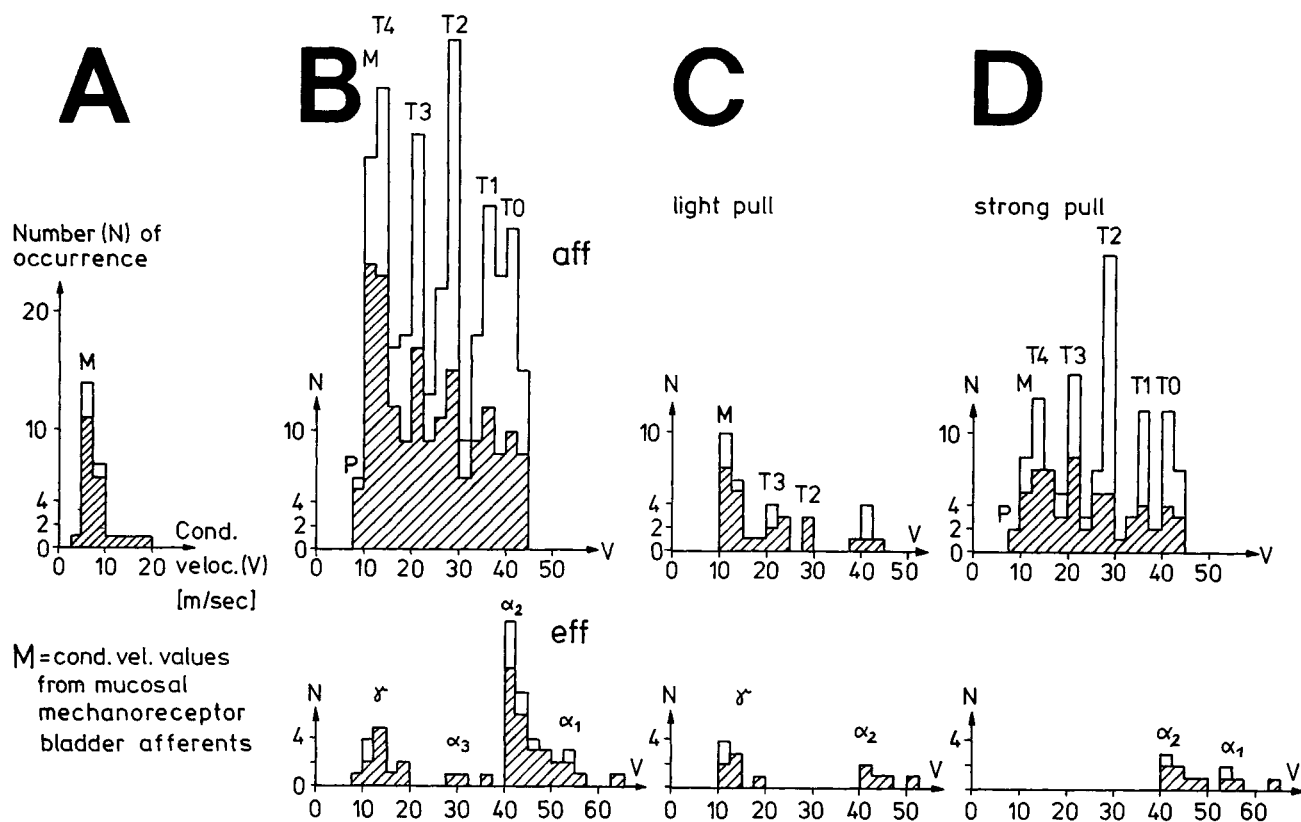


Fig. 6. — Conduction velocity distribution histograms of afferents from mechanoreceptors of the bladder (M) and skin (T0, T1, T2, T3, T4, P) stimulated by pulling a bladder catheter (upper part). Lower part, simultaneously measured efferents ( $\alpha_1$ ,  $\alpha_2$ ,  $\alpha_3$ ,  $\gamma$ ). A, recording from a dorsal S3 root, HT5. B, C, D, recording from a dorsal S4 root, HT6.

- A. Histogram from 2 recordings of single stimulations. Note the typical shape of a distribution peak from a single class of afferents.
- B. Sum of 4 histograms, each being the response to a single stimulation.
- C. Histogram from a single sweep of 1 light stimulation. Note that peak M has similar shape to the one in A.
- D. Histogram of a single sweep of 1 strong stimulation. In the efferent histogram the  $\gamma$ -motoneurons are missing, because high afferent activity masked them.

S3 dorsal root, one obtains a histogram with only one peak (Fig. 6A). This peak (M) is interpreted as the conduction velocity distribution of afferents from one kind of mechanoreceptors from the mucosa of the bladder. If one records from a more distal S4 dorsal root (Fig. 6B) one gets a histogram with many peaks. But all the additional peaks (T0, T1, T2, T3, T4) are the known skin afferent peaks. This histogram is therefore interpreted as originating from the stimulation of mucosal mechanoreceptors and skin mechanoreceptors of the pubic region and the ostium urethrae externus. The S4 root recording from a light stimulation (Fig. 6C) supports this view, since that histogram really only shows the M peak and is therefore similar to the recording of figure 6A,

probably because only a few skin receptors of the pubic region had been stimulated. A strong pull (Fig. 6D) probably gave a histogram with afferent peaks of the skin and mucosa because most possible regions had been stimulated.

Only afferent activity from the mucosa was obtained from the S3 recording and this can be interpreted in such a way that the S3 root innervated the mucosa of the bladder and the urethra, but not the pubic skin region and the ostium urethrae externus, whereas the S4 root did it at least partly. Indirect stimulations of other regions of the body, especially the perivesicular parts, cannot be excluded in the case of the strong catheter pull. It also seems as if the skin pain peak (P) occurred (Fig. 6B, D), but the separation from the M peak is not safe.

## Conduction velocity distributions from anal catheter stimulation

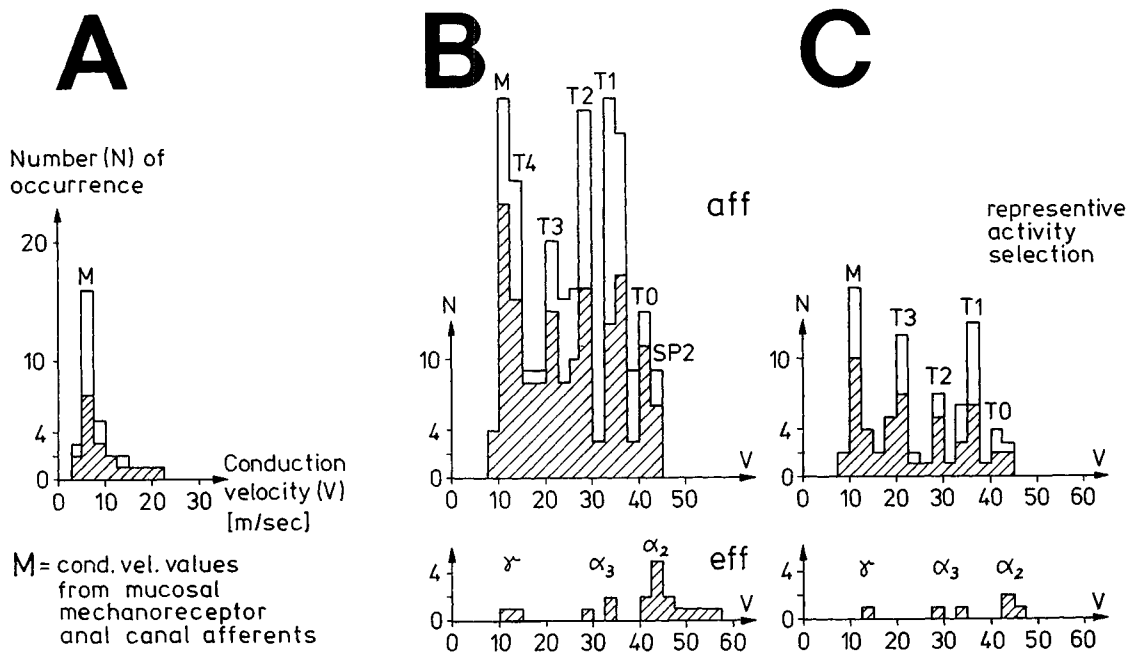


Fig. 7. — Conduction velocity distribution histograms of afferents from mechanoreceptors of the anal canal and perianal skin (M, T0, T1, T2, T3, T4) stimulated by pulling the anal catheter (upper part). Lower part, simultaneously measured efferents ( $\alpha_2$ ,  $\alpha_3$ ,  $\gamma$ ). A, recording from a dorsal S3 root, HT5. B, C, recordings from a dorsal S4 root, HT6.

- A. Histogram of 2 stimulations. Notice, same distribution shape as in figure 6A.
- B. Sum of 4 histograms, each of a single stimulation.
- C. Histogram from a single stimulation.

3.1.6. *Afferents from mechanoreceptors of the mucosa of the anal canal and the ampulla recti*

For the physiological stimulation of the mechanoreceptors of the anal canal and the ampulla recti, an anal catheter was used with the balloon in the ampulla recti. The stimulated areas were the ampulla recti, the anal canal and the perianal skin.

Figure 7 shows the conduction velocity distribution histograms constructed from the recordings of the activity increase due to the pulling of the anal catheter. The histograms of the figures 7A, B, and C can be directly compared with the ones of the figures 6A, B and C. They are very similar, only the skin afferent peaks do not disappear in the case of the slight catheter pull (Fig. 7C), indicating that there are

also skin mechanoreceptors present in the anal canal. Figure 7A shows the single peak of M afferents from the mucosal mechanoreceptors (S3 recording) and the figures 7B, C the histograms of mucosal afferents in connection with the skin afferents (S4 recording).

The segment interpretation is similar to the one of the bladder catheter stimulation (see discussion).

3.1.7. *Afferents activated by the retrograde filling of the bladder from a reservoir*

To record from afferents which inform the central nervous system about the filling stage of the urinary bladder, the bladder was continuously filled in a retrograde manner by gravity or light pressure with 0.9% saline solution of about 37°C through the bladder catheter from

Conduction velocity distributions stimulated by filling of bladder

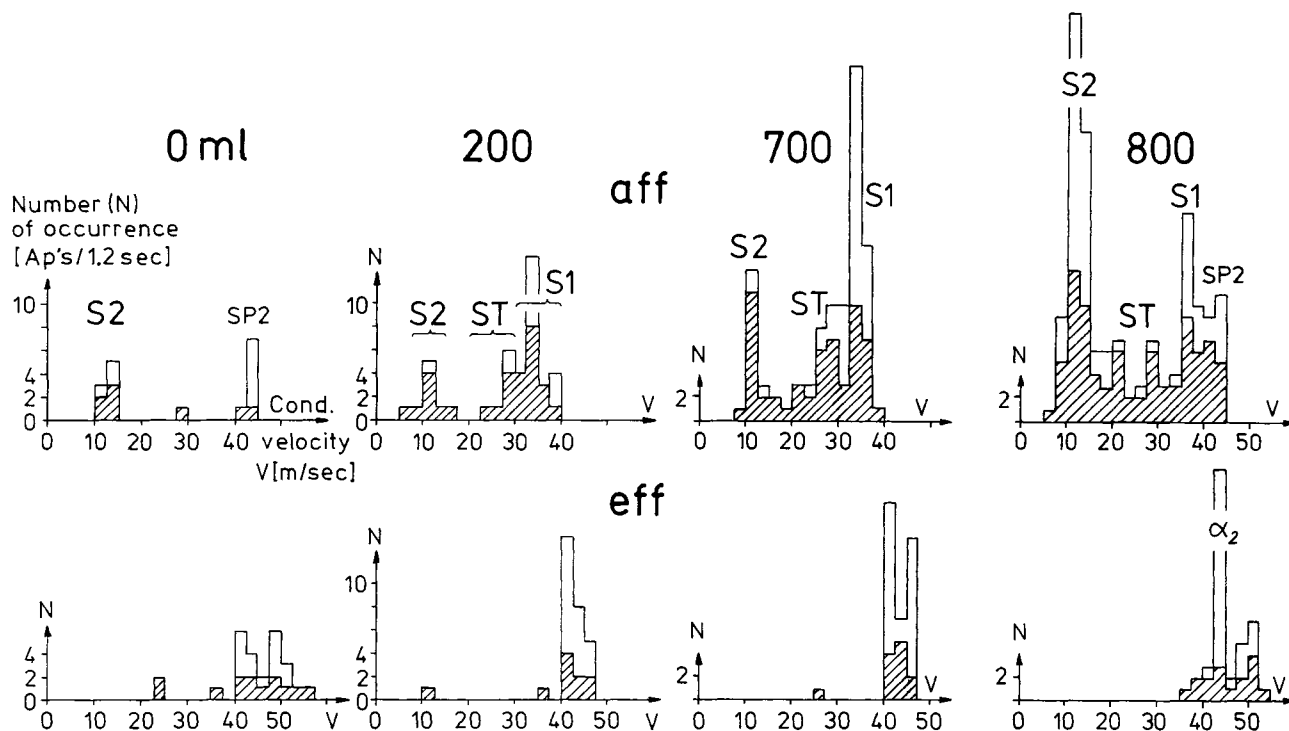


Fig. 8. — Conduction velocity distribution histograms of afferents from the urinary bladder receptors responding to the filling of the bladder (upper part). Lower part, simultaneously measured efferents. Afferent conduction velocity distribution peaks are marked with S1 ( $30 \text{ m/sec} \leq v < 40$ ), ST ( $20 \leq v < 30$ ) and S2 ( $7.5 \leq v < 15$ );  $v$  = conduction velocity. Dorsal S4 root recording, HT6. Speed of filling = 100 ml/min, 1 stop in between for root wetting. The histograms at 0, 200, 700 and 800 ml filling are the sum of 3 histograms, each constructed from a 400 msec sweep. Notice, the S2 peak is similar for 0 and 200 ml and increases with 700 and 800 ml, the S1 peak increases from 0 ml to 200 ml and is smaller for 800 ml.

a bag. The recorded activity was continuously stored on a tape and the filling stage was marked every 50 ml. Single sweep pieces are not very instructive and are therefore not demonstrated here (see Fig. 7B of Ref. 61). Since the activity varied quite a lot with the time, the activity from 3 sweeps of 400 msec were collected for the histograms shown in figure 8. The histograms at different stages in the filling of the bladder seem to show 3 peaks and they were marked with S1, ST and S2. The ST peak is less safe. At high "bladder-filling" stages (here 800 ml) it could be that other receptors outside the bladder contributed due to the pressure the bladder may have exerted on the surrounding tissue. It can be seen from figure 8 that the amplitude of the S1 peak increased from 0 ml to 700 ml and the afferent activity of that peak is interpreted as coming from stretch receptors of the bladder. The ST peak also

increased with the filling of the bladder and its activity probably originated from a second group of stretch receptors. The S2 peak showed different behaviour. This peak was already present when the bladder was empty and did not increase with the filling of the bladder up to about 600 ml. From 600 ml on, this peak increased strongly as can be seen from figure 8 (800 ml filling). To get more information about the receptors giving rise to that peak, the part of the filling of the bladder, where the filling procedure was stopped, was looked for. Figure 9 shows the activity peaks just before further filling of the bladder and just after. It can be seen that the S2 peak increased transiently very strongly, whereas the S1 peak was practically unchanged. The S2 receptors are therefore sensitive to fluid movements and high pressure in the bladder.

With the interpretation that the S2 receptors

### Change in filling of bladder (fluid disturbances)

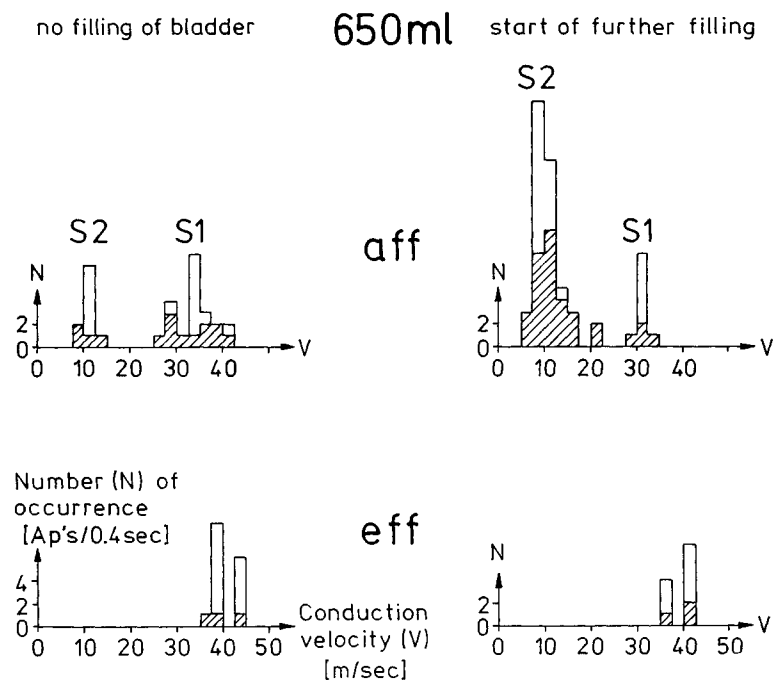


Fig. 9. — Conduction velocity distribution histograms for change in the filling of the bladder between 620 and 650 ml. Left, no filling; right, further filling started. S1, S2 afferent peaks are the same as in figure 8. HT6. Each histogram from a 400 msec sweep piece (1/3 of the time as in Fig. 8). Notice, the S2 peak changed very much with further filling; the S1 peak did not.

are mechanoreceptors (see discussion), the ever-present S2 activity can be explained by the mechanical stimulation which the bladder catheter exerted onto the urethra.

### 3.1.8. *Extrafusal ( $\alpha$ ) and intrafusal ( $\gamma$ ) motoneurons*

Three types of  $\alpha$ -motoneurons were identified in a previous paper (40) and are verified in this paper. Small corrections have to be made for the  $\alpha_1$ -motoneurons, supplying fast fatigue muscle fibres, as will be seen in the morphometry section.

$\gamma$ -motoneurons had not been observed in the previous paper. But in figure 3 and figure 4A conduction velocity distribution histograms of  $\gamma$ -motoneurons are shown. Even though one can see only 1 peak the actual measured velocities suggest that this peak consisted of 2 peaks, which were close together, as indicated in figure 3. In table 1, peak values of

$\gamma_1$  and  $\gamma_2$ -motoneurons are given. Wave forms of extracellularly recorded Ap's from  $\gamma$ -motoneurons are given in the second paper (41) in figure 4. A few efferents with conduction velocities between those of  $\gamma_1$  and  $\alpha_3$ -motoneurons were found in this measurement and are interpreted as  $\gamma_\beta$ -fibres. Their peak conduction velocity values are given in table 1 and figure 13.

The  $\gamma_\beta$ ,  $\gamma_1$  and  $\gamma_2$  intrafusal motoneurons could be renamed as  $\gamma_1$ ,  $\gamma_2$  and  $\gamma_3$  in similarity to the  $\alpha$ -motoneurons, where  $\gamma_1$ -motoneurons have the highest conduction velocity and the  $\gamma_3$  the slowest velocity. But since only a few measurements have been done on  $\gamma$ -motoneurons so far, the nomenclature will not be changed.

### 3.1.9. *Muscle spindle afferents*

Primary muscle spindle afferents (SP1) were identified in figure 3, with the assumption that they should conduct fastest among afferents,

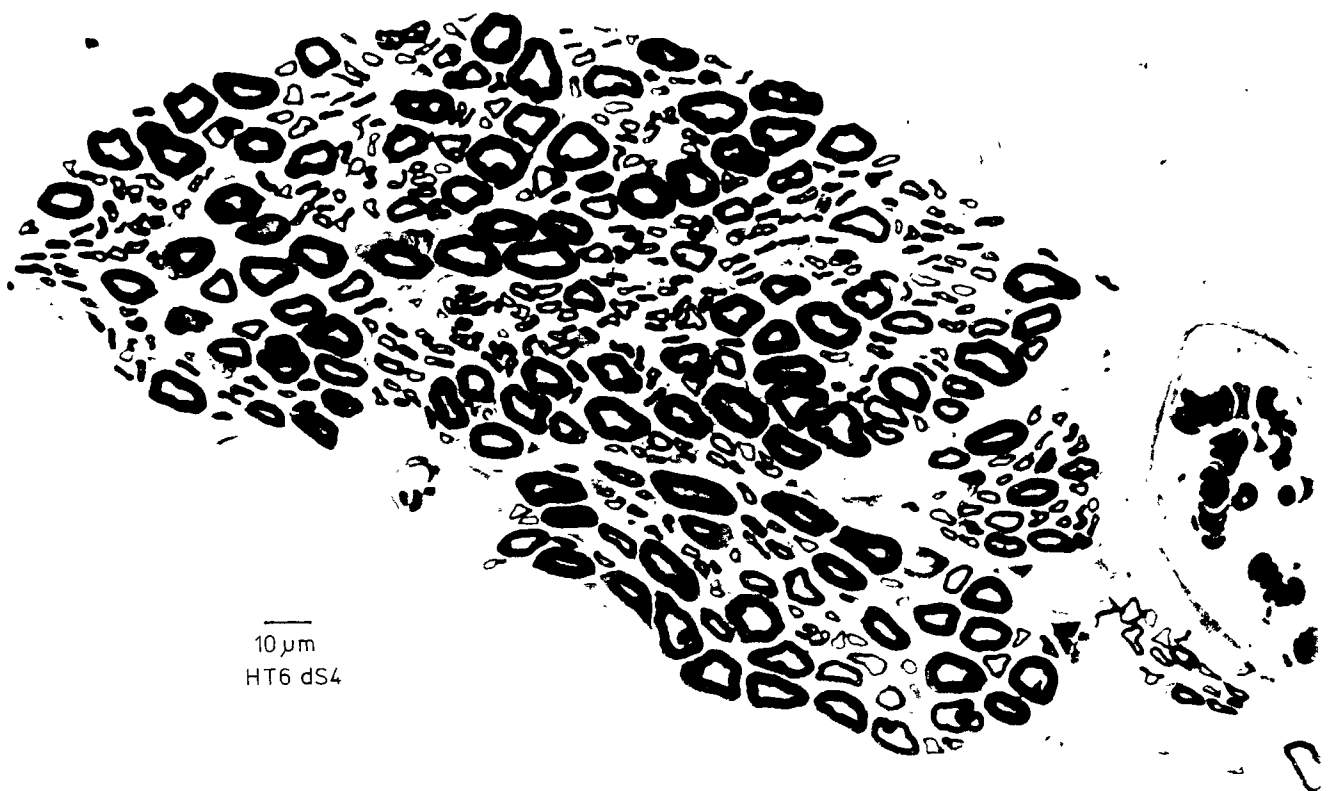


Fig. 10. — Light microscope photograph of a S4 dorsal root from the HT6. Thionin acridine-orange staining. Scale corrected for shrinkage. 4% glutaraldehyde fixation. Photograph contrasted with the copying-machine Minolta 450 zoom.



should have conduction velocities similar to those of  $\alpha_1$ -motoneurons and should be continuously active. Secondary spindle afferents (SP2) were identified with the assumption, that they should discharge rather continuously and that they should conduct slower than the SP1 fibres. Activity from Golgi tendon organ afferents have not been identified so far. But since there are perhaps no Golgi tendon organs in the external sphincters (no bony attachment) and the pelvic floor muscles are only activated a little (bladder and bowel empty, HT in the horizontal position), it is expected that only a few tendon organ afferent potentials are mixed with those of the other afferents. This rather weak identification of SP2 afferents gets functional support by the finding that these SP2 fibres change their activity in response to activity changes of the  $\gamma_1$  (dynamic) and  $\gamma_2$ -motoneurons (static) (42).

### 3.2. Morphometry

Root pieces were fixated and embedded for light and electron microscopy from the cadavers and from the HT's after the electrophysiological measurements. To correlate nerve fibre diameters with conduction velocities, the nerve fibre diameters and the myelin sheath thicknesses were measured by hand from the light microscope cross-sections like the one shown in figure 10 and nerve fibre diameter frequency distribution histograms were constructed for 3 myelin sheath thickness classes (d), as partly shown in figures 11 and 12.

With the help of a few known nerve fibre diameters and the electrophysiologically identified peaks it was partly possible to identify distribution peaks of nerve fibre groups in the nerve fibre diameter frequency distribution histograms. The shape of the diameter distribution of single afferent nerve fibre groups is assumed to be qualitatively the same as for efferent ones (Fig. 9 of Ref. 40). It seemed that the skewed non-gaussian distribution was sharper for the afferents. A schematic drawing of the distribution curve for fibre diameters and conduction velocities is given in figure 13, insertion. In

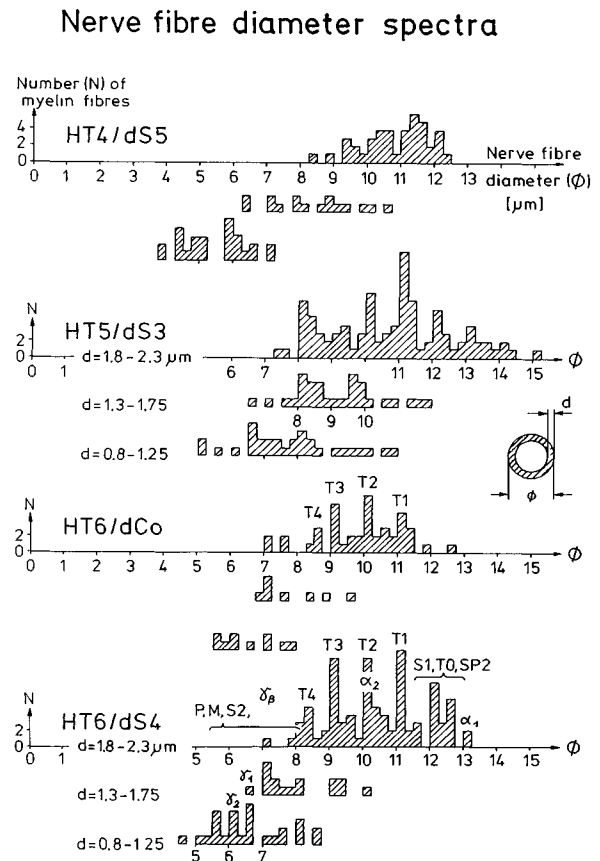


Fig. 11. — Nerve fibre diameter frequency distribution histograms from light microscope cross-sections like the one shown in figure 10. Each set, containing 3 histograms, is designated by the case (number of HT) and the root measured (d = dorsal, S = sacral, Co = coxygeal). The 3 histograms in each set are partly marked with the myelin sheath thickness range (d) of the nerve fibres, which are contained in it. T0, T1, T2, T3, T4 = touch afferent peaks, M = mucosal afferent peak, P = pain fibres,  $\alpha_1$ ,  $\alpha_2$  = extrafusal motoneurons,  $\gamma_\beta$ ,  $\gamma_1$ ,  $\gamma_2$  = intrafusal motoneurons.

comparison with the previous paper (40) the histogram classes were made smaller to increase accuracy, to separate peaks lying closer together. The disadvantage obtained with the smaller classes is that there were less fibres in each histogram class, so that the statistical variation increased.

From the electrophysiological measurements, it is known that in the dorsal coxygeal root (Fig. 11, HT6/dCo) there were most likely no efferents (probably below the level of motor nuclei) and no spindle afferents, since no effer-

ent potentials and no rather constantly firing afferents were observed. This dorsal root had therefore some similarity to a skin nerve. The first large peak ( $\varnothing = 11.2 \mu\text{m}$ ), when going from larger to smaller diameters, is therefore identified as the T1 peak, since the first main large peak when going from fast to slow conduction velocities of skin touch afferents is the T1 peak. This finding is in accordance with the largest peak in a skin nerve (Table 1, Cad 3, skin). The T2 (10.1  $\mu\text{m}$ ), T3 (9.1) and T4 (8.4) touch skin afferent diameter peaks were identified by counting the diameter peaks downwards according to the rule that in a first approximation a thicker nerve fibre has the higher conduction velocity, especially if rather similar nerve fibre groups are considered. Very similar

peak values could be found in other roots from the same HT (Fig. 11, HT6/dS4 and Fig. 12, HT6/dS3) and in other cases (Fig. 11 and 12).

The identification of the diameter peaks of the primary (SP1) and secondary (SP2) spindle afferents is started with the 2 peaks of largest diameter in figure 12 (HT6/dS3). The diameter peak at 13.2  $\mu\text{m}$  is taken as the SP1 peak, since the primary spindle afferents have the highest conduction velocity among afferents (Fig. 3) and probably also the thickest diameter. This identification is in accordance with the absence of the 13.1  $\mu\text{m}$  diameter peak in the histogram of the dS4 root of the HT6 (Fig. 11) where electrophysiologically, no primary spindle afferents could be found. The 2 fibres are most likely  $\alpha_1$ -motoneurons, since about 2 of them had been found electrophysiologically. The diameter peak at 12.1  $\mu\text{m}$  (Fig. 12, HT6/dS3) has been taken as the SP2 peak, since it is believed that SP2 fibres are also quite thick. This choice is supported by the existence of that peak in the dS4 (HT6) diameter spectrum, where several secondary spindle afferents had been electrophysiologically identified and by the absence of that diameter peak in the dC0 (HT6) spectrum, where no secondary spindle afferents could be found electrophysiologically. Uncertainty comes into this SP2 identification, since the fibres from the Golgi tendon organs have not been identified so far. For the S1 stretch afferents no fibre diameter can be given either. The few T0 touch afferents with a diameter of about 13.0  $\mu\text{m}$  (40) will not bring much disturbance.

Peak nerve fibre diameters for P, M and S2 afferents could not be identified. Their values probably lie between 5.5 and 8.2  $\mu\text{m}$ .

The diameters of the  $\alpha_1$ ,  $\alpha_2$  and  $\alpha_3$ -motoneurons were identified in the previous paper (40) and fit in well here. For the  $\alpha_1$ -motoneurons a small correction is perhaps necessary. It does seem that the main  $\alpha_1$ -motoneuron peak lies at 13.1  $\mu\text{m}$  (Fig. 12, HT6/vS3). The subpeak at about 12.3  $\mu\text{m}$  probably indicates a subgroup and is designated with  $\alpha_{11}$ . Subpeaks with diameters larger than 13.1  $\mu\text{m}$  could exist. Since there are only a few  $\alpha_1$ -motoneurons in the lower sacral nerve roots,

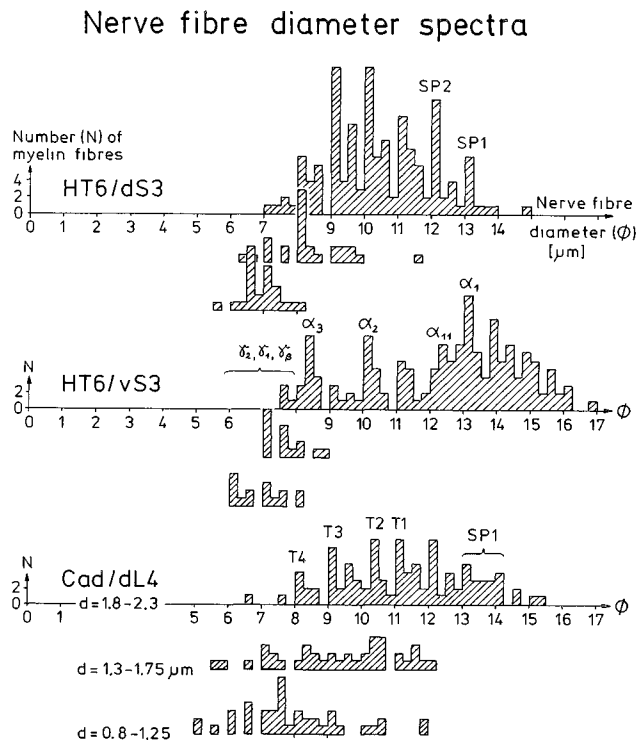


Fig. 12. — Nerve fibre diameter distribution histograms from light microscope cross-sections. Each set of 3 histograms is designated by the case (HT or Cad) and the root measured ( $d =$  dorsal,  $v =$  ventral,  $S =$  sacral,  $L =$  lumbar). The 3 histograms are partly marked with the myelin sheath thickness range ( $d$ ). T1, T2, T3, T4 = touch afferents; SP1, SP2 = primary and secondary spindle afferents;  $\alpha_1$ ,  $\alpha_{11}$ ,  $\alpha_2$ ,  $\alpha_3$  = extrafusal motoneurons;  $\gamma_\beta$ ,  $\gamma_1$ ,  $\gamma_2$  = intrafusal motoneurons.

not much information was obtained from them in these measurements.

In the electrophysiological measurements from the dorsal S4 root (HT6) intrafusal motoneurons ( $\gamma_\beta$ ,  $\gamma_1$ ,  $\gamma_2$ ) were identified. A scaling down, just by counting down, is perhaps unjustified, because there are also many afferent fibres (for example P, M, S2) in this diameter range. In the next section (Fig. 14) an extrapolation in the "conduction velocity — nerve fibre diameter" plane will be performed to get approximate nerve fibre diameters for  $\gamma_\beta$ ,  $\gamma_1$

and  $\gamma_2$ -motoneurons. According to this approximation, peaks at 7.2, 6.7 and 6.2  $\mu\text{m}$  in the diameter histogram HT6/dS4 (Fig. 11) are designated with  $\gamma_\beta$ ,  $\gamma_1$  and  $\gamma_2$ .

### 3.3. Correlation between electrophysiology and morphometry

#### 3.3.1. Summarized peak conduction velocity and peak nerve fibre diameter values

Table 1 summarizes peak values of conduction velocity distribution peaks from conduc-

case	root	peak conduction velocity [m/sec]											peak nerve fibre diameter [ $\mu\text{m}$ ]											root $\phi$ [mm]		
		P	M	S2	T4	T3	ST	T2	S1	T1	T0	SP2	SP1	P	M	S2	T4	T3	ST	T2	S1	T1	T0		SP2	SP1
		( $\alpha_2$ )			( $\gamma_1$ )	( $\gamma_\beta$ )		( $\alpha_3$ )				( $\alpha_2$ )	( $\alpha_1$ )	( $\gamma_2$ )	( $\gamma_1$ )	( $\gamma_\beta$ )	( $\alpha_3$ )		( $\alpha_2$ )				( $\alpha_1$ )	( $\alpha_1$ )		
Cad f 47	dL4 vL4																		8.2	9.1		10.3	11.1		12.2	13.3
																			(8.5)			(10.5)			(12.7)	
Cad3 m 64	I9 musc skin																								11.4	13.3
HT3 f 21	vS4				21	31		39		44	49	51													11.1	13
								(37)				(51)							(8.5)			(10.1)			(12.1)	0.15
33.5/36°C	L?	(15)			(20)							51	59												(50)	(60)
																										0.1
HT4 f 56	dS5	4	7		7	14		21		26	29															0.25
32/32.5°C						(14)		(21)				(29)							9.4			10.3	11.3			
HT5 f 58	dS3		6			14		19																		0.4
38/32°C								(12)											8.2	9.3		10.1	11.2			
HT6 f 37	dCo	5	--		6?	8		11		14	17								7.1 or 7.6	8.5	9.1		10.1	11.2	--	0.12
								(--)			(--)	(--)													(--)	
33.5/33°C																										
	dS4	9	12	12	14	21	28	29	34	36	41	43							5.5-8.2	8.4	9.1		10.1	11.1	12-12.7	0.2
		(10)			(14)	(20)	(30)					(43)							(6.2)	(6.7)	(7.2)				(13)	
	dS3																									0.3
	vS3																		(8.4)			(10.2)			(12.3)	(13.1)
	vL5																		(--)			(10.2)			(12.2)	(13.2)
Pat 24 m 10	dS?		5					20		25		30	43													
37/33°C?												(28.5)	(40)													

Table 1. — Peak conduction velocity values of conduction velocity distributions of single groups taken from conduction velocity histograms like those of figures 2, 3, 4, 6, 7 and 8 and peak nerve fibre diameter values of fibre diameter distributions of single identified groups taken from nerve fibre diameter histograms like those of figures 11 and 12 from 2 cadavers (Cad), 4 brain dead human cadavers (HT's) and one patient (Pat). Values without brackets are afferents, values in round brackets from efferents. T0, T1, T2, T3, T4 = touch stimulated afferents from skin and anal canal, P = skin pain afferents, M = touch afferents from the mucosa of the urinary bladder and the anal canal, S1, ST = stretch afferents of the bladder, probably measuring mural tension, S2 = flow receptor bladder afferents, stimulated by high pressure and fluid movements (may be identical with M), SP1, SP2 = primary and secondary spindle afferents. ( $\alpha_1$ ), ( $\alpha_{11}$ ), ( $\alpha_2$ ), ( $\alpha_3$ ) = extrafusal motoneurons, ( $\alpha_{11}$ ) = subgroup of ( $\alpha_1$ ). ( $\gamma_\beta$ ), ( $\gamma_1$ ), ( $\gamma_2$ ) = intrafusal motoneurons. (—), "—" = no peak present. f = female, m = male, number behind "f" or "m" is age in years, numbers below "f" or "m" are the central temperature and the temperature of the fluid in the spinal canal in °C. v = ventral, d = dorsal, L = lumbar, S = sacral, Co = coxygeal, I9 = 9th intercostal nerve, musc = muscle branch, skin = skin branch,  $\phi$  = diameter.

tion velocity frequency distribution histograms and identified corresponding peak values of nerve fibre diameter distribution peaks of the corresponding nerve fibre diameter frequency distribution histograms from all cases measured. Afferent and efferent (in round brackets) values are given in table 1 for the different nerve fibre classes. The nerve fibre values are quite constant for the different cases. But the nerve fibre conduction velocity values depend strongly on the temperature at the place of measurement. The temperatures measured were the central temperature and the one in the spinal fluid. The temperature in the nerve root, which is the most important one, was not known. With respect to the identification of nerve fibre groups, the problem was solved by

introducing the calibration relation of figure 3. To obtain conduction velocity values at a useful nerve root temperature, the values of the HT3 were used as a framework since the suggested temperature of the root was 36°C and the fastest values fit the measurements from Desmedt (17) and Buchthal (13). With the internal structure of conduction velocities of different nerve fibre groups from the other HT measurements, in figure 13 a conduction velocity family of afferents and efferents is constructed by interpolation at 36°C (human age about 30 years) with their corresponding nerve fibre diameters. The error of these mean values is probably not larger than ±10%, even though the variations in individual cases may be larger. Shifts of the peaks against each other must also be expected in the individual cases.

Conduction velocities (V) and diameters ( $\phi$ ) of afferent and efferent nerve fibres

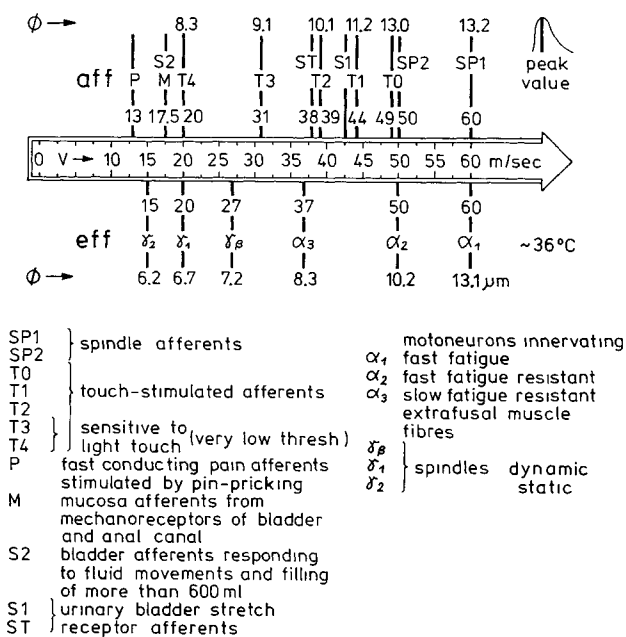


Fig. 13. — Approximate peak values of group conduction velocities (v) (root temperature 36°C) and group nerve fibre diameters ( $\phi$ ) of afferent and efferent nerve fibres in the cauda equina, human age about 30 years. S1, ST, S2, M, P = afferents, where the corresponding group nerve fibre diameters are not known. M, S2 = may be the same afferents. Insertion shows schematic frequency distribution shape of conduction velocities and nerve fibre diameters, peak value indicated.

### 3.3.2. Correlation between group conduction velocities and group nerve fibre diameters

Conversion factors from the conduction velocities to the nerve fibre diameters can be easily obtained from figure 13. But since these factors are different for each nerve fibre group, the conduction velocity and the nerve fibre diameter are given to characterize a group.

By comparing the conduction velocity and the nerve fibre diameter of afferent and efferent nerve fibre groups in table 1, one sees that they do not lie in the expected places with respect to a scaling down. For example the  $\alpha_3$ -motoneurons lie at the T2 touch afferent place in respect of the conduction velocity, but lie at the T4 touch afferent place in respect of the nerve fibre diameter. To show this property more clearly, conduction velocities and nerve fibre diameters of different  $\alpha$ -motoneuron and skin touch afferent groups were related in figure 14. It can be seen from figure 14 that the  $\alpha$ -motoneuron groups lie on a different correlation curve than the skin touch afferent groups. These correlations show that a single conversion factor from conduction velocities to nerve fibre diameters is not a good description of the reality. Extrapolating the  $\alpha$ -motoneuron correlation curve to smaller conduction velocity and nerve fibre diameter values, nerve fibre diameter values of

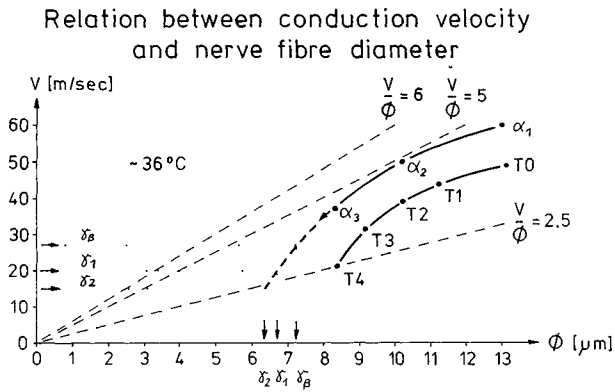


Fig. 14. — Relation between group conduction velocity and group nerve fibre diameter (peak values) of motoneurons and skin touch afferents in the “conduction velocity-nerve fibre diameter” plane at about 36°C (values taken from Fig. 13). Correlation curve of  $\alpha$ -motoneurons extrapolated to smaller values to obtain extrapolated  $\gamma$ -motoneuron diameters from the  $\gamma$ -conduction velocities.  $v/\phi$  = conduction velocity/fibre diameter. Notice, skin touch afferents and  $\alpha$ -motoneurons are not lying in the same “velocity-diameter” correlation curve.

$\gamma$ -motoneuron groups could be obtained from their conduction velocity values. These values obtained by extrapolation are given in figure 11 and table 1.

By looking at the correlation curves of the  $\alpha$ -motoneurons and the skin touch afferents in the “conduction velocity — fibre diameter” plane, it is obvious that the touch afferent fibres conduct slower at a given nerve fibre diameter. One possible reason for the reduced conduction velocity could be a thinner myelin sheath. But all  $\alpha$ -motoneurons and all skin touch afferents lie mainly in the myelin sheath thickness range  $d = 1.8\text{--}2.3\ \mu\text{m}$ . Therefore a different myelin sheath thickness may not be the main factor. There are probably differences in the axon membrane properties of skin touch afferents and  $\alpha$ -motoneurons.

### 3.3.3. Dependence of the conduction velocity on the temperature

Exact temperatures of the measured roots were not known. Absolute conduction velocity dependency could therefore not be calculated. But relative dependency could be studied since the 2 temperatures in figure 15, even though

### Temperature dependence of conduction velocities

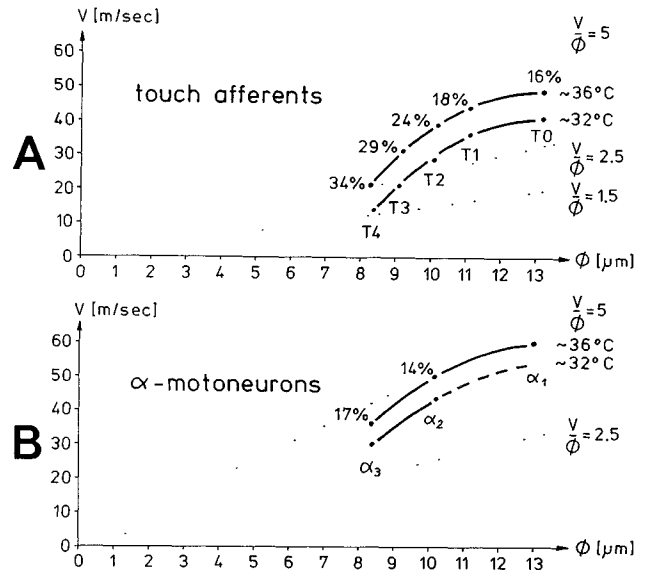


Fig. 15. — Temperature dependence of group conduction velocities (peak values) of skin touch afferents (A) and  $\alpha_2$  and  $\alpha_3$ -motoneurons (B). 36°C-trace from HT3, 32°C-trace from HT6. Temperature values are only very approximate. Percentages give the drop of conduction velocity values when changing from 36°C to 32°C.

only approximately known, were still the same for the  $\alpha$ -motoneurons and the touch afferent groups, because conduction times were measured simultaneously. In figure 15A the temperature dependence of the touch afferent groups change from 16%/4°C to 34%/4°C when going from the T0 group to the T4 group. This clearly indicates that in thinner touch afferents the conduction velocity depends more strongly on the temperature.  $\alpha_2$  and  $\alpha_3$ -motoneurons (Fig. 15B) show a similar behaviour, namely that the group with the thinner fibres and the lower conduction velocities are more temperature-dependent. Another observation from figure 15 is that the conduction velocities of the  $\alpha$ -motoneurons are about only half as dependent on the temperature than the touch afferents.

### 3.3.4. Number of efferents in dorsal sacral roots with fibre diameters larger than 5.5 $\mu\text{m}$

The calculated numbers of dorsal root efferent fibres are only very approximate since,

firstly, not all motoneurons may have been activated and, secondly, only approximate numbers can be obtained from conduction velocity distribution histograms (hatched part = each conduction velocity value taken only once). In a dorsal S3 root (HT5) 5 efferent fibres ( $2\alpha_2 + 1\alpha_3 + 2\gamma$ ) were found in 152 fibres (Fig. 11). A dS4 root (HT6) had 23 efferents ( $2\alpha_1 + 10\alpha_2 + 3\alpha_3 + 8\gamma$ ) among 125 fibres (Fig. 11) and a dS5 root (HT4) contained about 20 to 30% efferents (no ventral S5 root was existing). In a coxygeal root (HT6), no efferents could be detected, probably this rootlet was below the efferent level. A further dS3 root (HT6) contained efferents, but the number was not counted. Therefore, in all 4 dorsal sacral nerve roots efferent fibres could be detected electrophysiologically. Their percentage increased from 3% in the S3 root to 18% in the S4 root to about 20 to 30% in the S5 root. Only nerve fibre diameters which were larger than  $5.5 \mu\text{m}$  were taken into consideration. Even though variations in the lower sacral roots are frequent, these numbers indicate that the percentage of efferent fibres increases when going to the distal part of the conus medullaris. A possible explanation for this mixing in the conus medullaris is the closeness of rootlets, which is in the range of 1 mm or less.

### 3.3.5. Existence of SP1 afferents, $\alpha_1$ and $\gamma_\beta$ -motoneurons in the lower sacral roots

In the S3, S4, S5 and Co roots only few primary spindle afferents and  $\alpha_1$  and  $\gamma_\beta$ -motoneurons were found. It follows that these fibres are not important for urination and defecation. The external urethral and anal sphincters can only be innervated by  $\alpha_2$  and  $\alpha_3$ -motoneurons.

## 4. Discussion

### 4.1. Nerve fibre classification scheme

The classification of human nerve fibres in pairs "conduction velocity — fibre diameter" relies on the internal consistency of simultaneously measured conduction velocities and

nerve fibre diameters, the relative calibration of conduction velocities by correlating the velocities of afferent and efferent fibres (Fig. 3) and on the absolute calibration of conduction velocities by comparing the conduction velocity values of the distribution peaks of the  $\alpha_1$ -motoneuron and the primary spindle afferent groups with the fastest conduction velocity values obtained from compound action potential (Ap) measurements of afferent (4) and afferent and efferent fibres (17). The accuracy of the internal consistency is high since afferent and efferent conduction velocities and diameters of different fibres were measured under the same conditions for each case (root). Slight temperature shifts could have entered the measurement of the HT6 because of the long measuring time (filling of the bladder). An error of 5 to 10% could have entered the absolute calibration, since it is not clear whether the fastest conduction velocity values measured from compound Ap's are the distribution peak values of the fastest conducting group or higher values. In the schematic drawing of figure 13 a round and simple conduction velocity value of 60 m/sec is given for the  $\alpha_1$ -motoneurons and the primary spindle afferents. Behse and Buchthal (4) measured the max. sensory velocity as 3 to 6 m/sec faster than the max. motor velocity. Also the measurement from the patient (Pat 24 in Table 1) may indicate that the primary spindle afferents conduct slightly faster than the  $\alpha_1$ -motoneurons.

A direct comparison of the measured pairs "conduction velocity — fibre diameter" with existing values is not possible, since such accurate pair values do not exist for humans nor for animals. A list of measured conduction velocities from many authors (51) is not of much help, since those values were from different species, different measuring procedures were used, mostly only ranges of conduction velocities were given (no peak values) and little is said about whether the measured conduction velocity ranges were representative selections. In the following, single nerve fibre classes will be compared with human values and, if they are not available, with animal data. If animal data are used it will be stated explicitly.

#### 4.2. Nerve fibre identification with respect to conduction velocity and fibre diameter distributions

As has been shown for  $\alpha$ -motoneuron diameters (Figs 8, 9 of Ref. (40)) and conduction velocities of mucosal afferents (M) (Figs. 6A, 7A) a class of nerve fibres is most likely characterized by conduction velocity and fibre diameter distributions. The given values here are the peak values of such skewed distributions (Fig. 13, insertion). Since velocity and diameter distributions of groups overlap, it is possible for example to find an  $\alpha_3$ -motoneuron in the  $\alpha_2$ -motoneuron class range or a T2 afferent fibre in the T1 class range. A rather safe characterization of a fibre class is possible by giving the velocity, the diameter and the function.

#### 4.3. Types of mechanosensitive units of the skin

Disregarding the small peak of T0 afferents, 4 types of touch afferents, T1, T2, T3 and T4 (Fig. 2), have been identified from the nearly hairless skin on top of the gluteus maximus (S3 to coxygeal dermatomes). 4 different types of mechanosensitive units with low threshold have been identified from the glabrous skin (48, 53, 55). The interpretation is (48) that the end organs of the 4 types of units are paciniform nerve endings for the PC units, Meissner's corpuscles for the RA units, Merkel's cell neurite complexes for the SAI units, and Ruffini's nerve endings for the SAI units. It is quite clear that the PC, RA, SAI and SAI units are identical to the T1, T2, T3 and T4 touch units, it is not clear, which is which. There is indication in this paper, that the T1 and T2 units adapt more rapidly than the T3 and T4 touch units. The T1 and T2 units therefore correspond to the PC and RA units (rapidly adapting) and the T3 and T4 units to the SAI and SAI units (slowly adapting). The lower part of figure 5A, including the insertions "1" and "2", indicates further that the 3 T1 units come from 3 different points and have no distinct receptive field borders and also signal the accel-

eration of skin indentation (see the calculations in connection with the delays). The T1 units are therefore most likely the PC units with the single pacinian corpuscles. The pacinian corpuscles are innervated by thick myelinated nerve fibres and are also quite often present, similar to the T1 units (Fig. 2A, Fig. 11, HT6/dS4). Maybe SAI units have a slower conduction velocity than the SAI units (55) and correspond to the T4 units. A safe correlation of the different units on the basis of their conduction velocities (54, 55) is not possible, since figure 1 and figure 5 demonstrate that the delays from the moment of touching the skin to the appearance of the Ap's, used by Knibestöl (54), are not always in relation to the conduction velocity of the fibre. PC, RA, SAI and SAI units are probably the T1, T2, T3 and T4 units respectively.

The function of the T0 unit is unclear. But the small distribution peak seems to be more than just misjudged secondary spindle or golgi afferents. Since in the hairy skin only one additional hair follicle unit could be identified (48), it seems that the T0 afferents innervate hair follicles. This interpretation is supported by the finding that in the cat the fastest conducting mechanoreceptive units come from the hair follicle type T(12) units, but hair follicle afferents are much more important and different in the cat than in the human. The afferents from the hair follicles are still unclear, since in the measured areas also down hair (thin blond short hair, directed more downwards) may have been stimulated in addition to the pubic hair.

The conduction velocity distributions of the touch afferent groups measured in this paper have similarity with those of the cat (12, 24), only the peak velocity values have to be reduced by about 30 to 35%.

The peak conduction velocity of myelinated pain afferents (high-threshold mechanoreceptor afferents of  $A_\delta$  type in the Erlanger and Gasser classification) is 13 m/sec. The peak fibre diameter is in the range between 5.5 and 8.2  $\mu\text{m}$ . A conduction velocity distribution histogram from nociceptive  $A_\delta$  afferents of the cat (14) has its peak at about 18 m/sec (range from 6 to

37 m/sec) and shows nicely the typical skewed distribution of figure 4B and figure 13, insertion, with the "long foot" to the higher values. The peak conduction velocity value reduced by 30% fits approximately the human value of 13 m/sec.

#### 4.4. *Afferents from the urinary bladder and the anal canal*

In the cat afferents have been identified in the pelvic nerve and hypogastric nerve responding to tension changes in the detrusor musculatur and mechanical distension of the mucosal-submucosal surface (52). The tension afferents conducted below 16 m/sec and the mucosal mechanical afferents between 18 and 22 m/sec. It is possible that these afferents correspond to the S2 and M afferents respectively, which both had conduction velocities of 12 m/sec at  $\sim 32^\circ\text{C}$  and 17.5 m/sec at  $36^\circ\text{C}$  (corrected). Todd (47) measured indirectly from cat pudendal nerves by recording from fine strands of sacral dorsal roots and cutting all branches of the sacral plexus, except those giving rise to the pudendal nerves. Distending the urethra with fluid, he recorded discharges of large amplitude, that means from rather thick and fast conducting afferents (39). The receptors of these afferents were not sensitive to the flow of saline solution along the urethra and are therefore probably similar to the stretch receptors S1 and ST (Figs. 8, 9). When the urethra was obstructed by a ligature a steady stream of fluid along the urethra was accompanied by action potentials of low amplitude (from thinner, more slowly conducting fibres) which increased in frequency especially when the flow started or its rate was changed (compare with Fig. 9). The afferents from these flow receptors are most likely the S2 afferents (Figs. 8, 9). Todd (47) argued that the flow receptors are probably rapidly adapting mechanoreceptors which respond to higher fluid velocities, when the laminar flow breaks down into turbulent flow. It seemed to him that the turbulence in the flow represents the normal mode of stimulation of the flow receptors. Irregularity

of the wall or narrowing of the lumen ought to increase the possibility of local turbulence. Small lamelled end-organs were found in the most superficial layers of the urethral mucosa at the summits of mucosal folds with the long axis parallel to the direction of flow (47).

The S1 and ST afferents are most likely stretch receptors, which probably monitor tension, since their activity increased with the filling of the bladder (Fig. 8) and decreased when the filling of the bladder was stopped (Fig. 9 of Ref. 41), a stage when the bladder adapts and the pressure reduces (62). The conduction velocity distributions suggest that there are 2 stretch receptor populations, even though a subgrouping of one receptor kind cannot be excluded. But since the ST afferents seem to start to respond a bit later with increasing filling of the bladder (Fig. 9 of Ref. 41), it is conceivable that the ST (stretch-tension) afferents have to secure overstretch of the bladder in similarity to the function of the golgi tendon organ afferents in skeletal muscle. The S2 afferents responded to fluid movements and high pressure (Figs. 8, 9; Fig. 9 of the second paper (41)). It is possible that Todd's (47) specialised mechanoreceptors which responded to fluid disturbances also respond to high pressure. But it is also likely that the S2 conduction velocity distribution population originated from two afferent populations, one responding to flow and the other to high pressure in the bladder. Also the mechanoreceptor afferents M of the bladder mucosa, responding to pulling of the bladder catheter, could be identical to all the S2 afferents or the part of them, which responded to high pressure, since they have the same peak conduction velocity.

The mechanoreceptor interpretation of the S2 flow receptors is in accordance with human feeling. If one lets a drop of water run along the skin or lets water stream alongside the skin while sitting in the bath-tub one can experience a feeling similar to the beginning of micturition when the urin enters the proximal urethra. The flow of fluid at the skin is probably registered by the very low-threshold mechanoreceptors T3 and T4 (sensitive to very light touch). The S2 afferents responding to flow in the urethra and



trigonum vesicae will not give rise to exactly the same feeling as the T3 and T4 afferents of the skin, since the S2 afferents probably have different receptors may have a different firing pattern and probably are connected differently in the central nervous system.

With receptors for stretch (S1) and maybe overstretch (ST) and one or two mechanoreceptors (S2, M) for urine flow, touch and high pressure, the bladder has an elaborate sensory system for monitoring its functional stage.

The impulse pattern of the S1, ST and S2 afferents were more burst like than continuous. With the turbulence interpretation (47), this can be expected for the flow receptors. But also the stretch afferents, probably monitoring tension, could respond more burst-like, since Iggo (26) suggested that bladder tension-receptors are "in series" with the muscle fibres. Also in a continuously stretched bladder, due to the continuously retrograde filling of the bladder, the stretch receptor firing patterns could be irregular.

It seems as if there was also some pain activity recorded from the bladder wall and the urethral wall, since the skin pain peak seemed to occur with strong pulling of the bladder catheter (Fig. 6B). Patients report pain with strong bladder catheter pulling. Touch and pin-pricks during cystoscopy are interpreted as pain in the bladder and also in the prostatic urethra (6, page 154).

By pulling the anal catheter the conduction velocity peaks of the 5 skin touch afferent classes and one additional M peak were obtained (Figs. 7B, C). This was to be expected, since the lining membrane of the anal canal in man contains all the skin modalities (18). The sensitivity seemed to be more acute than in the majority of cutaneous surfaces (18). Duthie and Gairns (18) found additionally, a profuse innervation with a highly specialised receptor in the lining membrane of the anal canal, which probably gave rise to the activity of the M afferents. But they did not find these receptors in the mucosa of the rectum. It still seems that there are M mechanoreceptors in the mucosa or submucosa in the caudad rectum or, at least, at the transition zone from the anal canal to the rectum (transitional-columnar epithel junction),

since figure 7A shows a velocity distribution from afferents only from the additional mucosa receptors.

This sensory innervation of the anal canal with its important role in preserving continence, can be understood. When the rectum is distended by contents, the fullness is probably sensed by the receptors of the M afferents, not allowing a discrimination between flatus and feces. Reflex relaxation of the internal sphincter and contraction of the external sphincter occur with further rectal distension and permit momentary contact of the rectal contents with the sensitive epithelial lining of the anal canal; this provides warning of the presence of the material and permits discrimination of its nature since the additional mechanoreceptors T1, T2, T3 and T4 have different thresholds so that probably the relative high threshold Pacinian corpuscles of the T1 afferents, lying deep in the region of the muscle bundles (56), are only stimulated by feces but not by flatus. Voluntary control or differential passage of flatus or feces is therefore possible.

By comparing figure 6C with figure 7C one can see, that with a light pull of the bladder catheter there are not so many kinds of skin afferents which are stimulated simultaneously with the mucosal afferents as with the pull of the anal catheter (S4 root recording). It indicates that in the urethra there are no, or not so many skin-like receptors as in the anal canal. This can be understood with the above interpretation. The receptors of the urethra need not to distinguish between different contents; only urine normally passes through. Even though they are of the same cloacel origin (6, page 7) the urethra and the anal canal probably differentiated a bit differently according to the contents they transport.

The S3 dorsal root recording of the HT5 in figure 6A and figure 7A shows only mucosa mechanoreceptor afferent activity from the bladder, anal canal and rectum indicating little overlap of the S3 segments with the ones of S4 and S5. But Bohm (5) reported a large variation of the area and overlap of the S2 to S5 segments, therefore large variations of the lower sacral segments have to be expected. This

is similar to the very large dermatome overlap from S3 to S5 experienced in these measurements.

The conduction velocity distributions from the afferents of low-threshold mechanoreceptors of the bladder (M) and the anal canal (M) are very similar. It seems possible that these afferents have the same receptor type. More functional aspects of afferents and efferents of bladder and anal canal will be discussed in the following two papers (41, 42).

#### 4.5. Spindle afferents

Primary spindle afferents have seldom been observed in the lower sacral nerve roots (Table 1 of Ref. 40). It is probable, that the muscle spindles in this range have practical no primary afferents. It has been reported in the case of the cat, that the nerve supply of muscle spindles varies (7) and not much is known about the spindles in the sphincters or in the pelvic floor muscles. In the cat muscle spindles are present in the external anal sphincter. The existence of muscle spindles in the external urethral sphincter is unclear (see second paper (41)). The conduction velocity value of primary spindle afferents is given in figure 13 with 60 m/sec, which is the same value as for  $\alpha_1$ -motoneurons. Table 1 suggests that the primary spindle afferents conduct a bit faster than the  $\alpha_1$ -motoneurons. For the explanation of the H-reflex, it is assumed that primary spindle afferents are stimulated before the  $\alpha_1$ -motoneurons with increasing current strength. But because there could be axon membrane differences between the  $\alpha_1$ -motoneurons and the primary spindle afferents, the excitability order is not conclusive for small differences in the conduction velocity. So as not to demonstrate an accuracy which may not exist, the conduction velocity values of the  $\alpha_1$ -motoneurons and primary spindle afferents are given with round values of 60 m/sec. Conduction velocity values of Golgi tendon organ afferents probably lie between those of primary (60 m/sec) and secondary spindle afferents (50 m/sec). The highest values are reported to be of 56 m/sec (58).

The functional relation between secondary spindle afferents (SP2) and motoneurons will be analysed in the second (41) and third paper (42). The mean activity of a secondary spindle afferent fibre (SP2<sub>1</sub>-fibre in Fig. 8D of the second paper (41)) was about 13 Ap's/sec and the highest activity values of SP2-fibres, reached with different bladder and anal canal stimulations were nearly 10 Ap's/sec per fibre (Fig. 6, 7 of the third paper (42)). These activity levels are compatible with the one of the stretch response of human intercostal muscle spindle secondary afferents, which are about 12 impulses/sec per 5% extension (36).

#### 4.6. $\alpha_1$ , $\alpha_2$ and $\alpha_3$ -motoneurons (extrafusal)

In the previous paper (40) the  $\alpha$ -motoneuron classes were identified by their peak conduction velocity and peak nerve fibre diameter values at about 37°C:  $\alpha_1$ (61.5 msec<sup>-1</sup>/12.5  $\mu$ m),  $\alpha_2$ (49/10.3),  $\alpha_3$ (37.5/8.3). They are innervating fast easily-fatigued muscle fibres (FF), fast fatigue-resistant muscle fibres (FR) and slow fatigue-resistant muscle fibres (S) respectively. The velocity-diameter pairs measured in this paper are at a temperature of ~36°C:  $\alpha_1$ (60 msec<sup>-1</sup>/13.1  $\mu$ m),  $\alpha_2$ (50/10.2),  $\alpha_3$ (37/8.3). The new values are in good agreement with the former ones. Only the peak nerve fibre diameter of the  $\alpha_1$ -motoneurons seems to be larger, with a value of 13.1  $\mu$ m, and there seems to exist a subgroup of the  $\alpha_1$ -motoneurons, the  $\alpha_{11}$ -motoneurons, with a peak nerve fibre diameter of 12.2  $\mu$ m (Fig. 12, HT6/vS3; Table 1). For histochemical muscle fibre types see reference 3.

It does seem from the fibre diameter distribution of figure 12 (HT6/vS3) that there may be even more subgroups at higher values than the main  $\alpha_1$ -peak. The  $\alpha_{11}$ -motoneurons (?/12.2  $\mu$ m) are probably the subgroup of the  $\alpha_1$ -motoneurons (FF-type) prominent in the lower sacral nerve roots, which corresponds to the intermediate-fatigue type (F(int)) of motoneurons in cats (28). A conduction velocity identification of the  $\alpha_1$ -motoneurons, along

with its probable subgroups, in the lower sacral nerve roots is not possible, since there are only a few  $\alpha_1$ -motoneurons in these roots.

Cat peak conduction velocities and nerve fibre diameters of  $\alpha$ -motoneurons (7, 10), not splitted up into  $\alpha_1$  and  $\alpha_2$ , are between 75 and 80 m/sec and between 13 and 14  $\mu\text{m}$ ;  $\alpha_3$ -motoneurons may not always be present in the lumbal range (Table 1, HT6/vL5 (40)). The human motoneurons conduct about 25-30% slower. Burke et al. (15) measured musculus gastrocnemius conduction velocities of  $\alpha$ -motoneurons innervating muscle fibres of type FF, FR and S from 100 to 85 m/sec in the cat.

The classification of the  $\alpha_1$ -motoneurons into 3 groups is strongly supported by the finding of the second paper (Table 1(41)), namely that each class of motoneurons has firstly its own membrane property of repetitive activity and, secondly, they are driven by their own spinal oscillators in the high activity mode (rate coding (46)).

#### 4.7. $\gamma_\beta$ , $\gamma_1$ and $\gamma_2$ -motoneurons (intrafusal)

The motoneurons innervating the muscle spindles are identified by their conduction velocity distributions, which can partly be seen in the figures 3, 4 and 6. Original recordings of the  $\gamma_1$  and  $\gamma_2$ -motoneurons can be seen in figure 4 of the second paper (41). The  $\gamma_2$ -motoneurons have a smaller Ap amplitude than  $\gamma_1$ -motoneurons and the  $\gamma_1$ -motoneurons have a smaller Ap amplitude than the  $\alpha_3$ -motoneurons (Fig. 4 of the second paper (41)). This Ap amplitude relation is the same as between the tonic and rhythmic  $\gamma$  and  $\alpha$ -motoneurons in the intercostal muscles of the cat (16). To obtain nerve fibre diameter peaks for the 3  $\gamma$ -motoneuron classes it was assumed that they have similar membrane properties than the  $\alpha$ -motoneurons. In the velocity-diameter plane the correlation curve of the  $\alpha$ -motoneurons was extrapolated towards  $\gamma$ -motoneuron values (Fig. 14) and the peak nerve fibre diameters were obtained from the peak conduction velocities by using the correlation curve (Fig. 14). For these extrapolated diameters, peaks could be

found in the fibre diameter distribution histogram of figure 11 (HT6/dS4).

The Ap's of  $\gamma_\beta$ -motoneurons had amplitudes and durations which lay between those of the  $\alpha_3$  and  $\gamma_1$ -motoneurons. The conduction velocities were also intermediate (Fig. 13). These  $\gamma_\beta$ -motoneurons were thought to be of intrafusal type, because of the general belief (8, 9, 46) and because of the formal view that if there exist 3 extrafusal motoneuron classes, it could be that there exist also 3 intrafusal motoneuron classes. This assumption is supported a bit by the finding that there are only few  $\alpha_1$  and  $\gamma_\beta$ -motoneurons in the lower sacral nerve roots (and also primary spindle afferents), both of which are supposed to be of a fast type. Functional support cannot be given for this classification, since only a few  $\gamma_\beta$ -Ap's were observed.

The possibility that  $\gamma_\beta$ -motoneurons innervate extrafusal and intrafusal muscle fibres is unlikely, apart from exceptions, since this would mean that an axon could be fast (conducting) and dynamic (response) with respect to intrafusal muscle fibres and slow and static with respect to extrafusal muscle fibres if the intrafusal muscle fibres also consist of different types. In figures 3 and 4 of the third paper (42) it will be shown that the  $\alpha_3$ -motoneurons are more static and unspecific in activity level changes, that the  $\alpha_2$ -motoneurons are more dynamic and specific, and that there is some indication that the  $\gamma_1$ -motoneurons are more dynamic and that the  $\gamma_2$ -motoneurons are more static (Figs 4, 7 of Ref. 42). In frogs, fast conducting axons (high regeneration speed) innervate extrafusal twitch muscle fibres (fast conducting, small membrane time constant) and slowly conducting axons (low regeneration speed) slow muscle fibres (slowly conducting, large membrane time constant). Only during metamorphosis (57) and regeneration (34, 43, 44) is there transient mixing. The fast regenerating axon population innervates transiently twitch and slow muscle fibres before the old pattern is reestablished with the arrival of the slowly regenerating, slowly conducting axons. It has been reported that single  $\beta$ -fibres innervate extrafusal and intrafusal muscle

fibres (59, 60, cat). If this holds also true in human than this would mean, that intrafusal muscle fibres are not or not so much grouped into different types.

The classification scheme of identifying a nerve fibre by the conduction velocity, the fibre diameter and the function holds true for the cauda equina and roughly for the peripheral nerves, but it does not hold true for, the place where the motoneurons split up into different branches. In axon branches the conduction velocity and the nerve fibre diameter have no meaning, since they are reduced with respect to the mother fibre. The  $\gamma_\beta$ -motoneurons spoken of in this paper, are the ones existing in the nerve roots as separate fibres.

The dynamic  $\gamma_1$ -motoneurons have a peak conduction velocity of 20 m/sec and a fibre diameter of 6.7  $\mu\text{m}$  (Fig. 13). Cat peak values are between 30 and 35 m/sec and between 6.5 and 7  $\mu\text{m}$  (7, 10). It seems that the velocity-diameter characterization of the  $\gamma_1$ -motoneurons at 36°C with (20 msec<sup>-1</sup>/6.7  $\mu\text{m}$ ) is quite good when one takes into account a 30% reduction of the conduction velocity.

The identification of the static  $\gamma_2$ -motoneurons is quite uncertain. Since their Ap's (Fig. 4C of Ref. 41) could quite often only be separated with difficulty from the noise and artefact level, it can be assumed that Ap's of very low amplitude from slowly conducting  $\gamma_2$ -motoneurons were lost in this noise and artefact level. The  $\gamma_2$ -motoneurons from figure 13 (15 msec<sup>-1</sup>/6.2  $\mu\text{m}$ ) could be a slowly conducting subgroup of the  $\gamma_1$ -motoneurons. The slower time course of their activity response (Figs. 4 and 7 of the third paper (42), region  $\gamma_2 > \gamma_1$ ) supports the case that they constitute the fast part of the  $\gamma_2$ -motoneurons. It is to be expected that the values of the whole class are a bit smaller than the values given in figure 13. Cat peak values of the  $\gamma_2$ -motoneurons are between 15 and 30 m/sec and between 3.5 and 4  $\mu\text{m}$  (7, 10). But it has also been reported for cats that the conduction velocities of dynamic  $\gamma$  and static  $\gamma$ -axons overlapped extensively (range: 15-55 m/sec) (9).

In cats (7), 45% (with large variations) of the motor fibres are, on average, intrafusal

with, on average, 2.9 fusimotor fibres per spindle, that means about 1 muscle spindle per 3 extrafusal motoneurons. Also in human there exists about one muscle spindle (with large variation) per 3 motor units (14). From the nerve fibre diameter spectrum of figure 12 (HT6/vS3), it can be calculated that about 15% of the motoneurons are intrafusal (at least 6 motor fibres per spindle). The nerve fibre diameter distribution histograms of figures 8 and 9 of reference 40 also suggest, that the percentage of intrafusal motoneurons in the lower sacral roots is lower than in the lumbal range. That not all  $\gamma_2$ -motoneurons were detected in this measurement, cannot account for the low percentage of intrafusal motor fibres, since, in the case of the cat (7), there are about twice as many  $\gamma_1$  than  $\gamma_2$ -motoneurons (7). In the cat, muscle spindles were found in the external anal sphincter, but not in the external urethral sphincter (47). Differences in the lower sacral roots in comparison to lumbal roots have to be expected.

#### 4.8. *Structural differences among myelinated nerve fibres*

From figure 14, it can be seen that the relation between conduction velocity and fibre diameter changed from thicker to thinner fibres and these changes were different for the 3  $\alpha$ -motoneuron classes and the 5 touch afferent classes. The temperature dependence of the  $\alpha$ -motoneurons and touch afferents of figure 15 corresponded to these changes. The temperature dependence increased as group conduction velocities became smaller, but, again, this was differently for  $\alpha$ -motoneurons and touch afferents. How the primary and secondary spindle afferents lie in the velocity-diameter plane is unclear, since the group fibre diameter of the SP2 fibres is uncertain. That the  $\alpha$ -motoneurons are derived from bipolar nerve cells and the touch afferents from pseudo-unipolar nerve cells, may be one reason for the different nerve fibre properties. But even among the  $\alpha$ -motoneuron classes there seem to be differences in the axon membrane properties and the relative

thickness of the myelin sheath, which cannot be explained just by a scaling-up factor (27). It has been shown in the cat (2), and suggested in human (40) that thicker axons have a comparable thin myelin sheath. As can be seen from table 1 of the second paper, the  $\alpha_2$  and  $\alpha_3$ -motoneurons show a different repetitive activity. In the cat, it has been shown that the input resistance and the rheobase (threshold depolarization) are different for the different  $\alpha$ -motoneuron classes (20, 22).

## 5. Clinical implications

### 5.1. *Conduction velocities and nerve fibre diameters in the use of clinical research*

In Restorative Neurosurgery it is necessary to connect nerves with respect to function (see second paper (41)). For a reconnection, it is necessary to know the circuitry and function of the peripheral nervous system (PNS) and partly of the central nervous system (CNS) of the human body with respect to microanatomy, nerve fibre compositions and activity patterns, and partly to verify these during an operation. With morphometrically identified peak diameters of certain nerve fibre groups, it is, for example, possible in cadavers to clarify partly the composition and function of small nerves, which branch and fuse, leading to the urinary bladder, prostate and sexual organs. In areas or cases, where it is also possible to record extracellular action potentials (Ap's) with 2 pairs of electrodes, nerve fibre groups can additionally be identified from conduction velocity distribution histograms under different stimulation conditions. The Ap pattern of single nerve fibres can be followed up in the complex afferent and efferent impuls traffic in the undamaged nervous system by identifying nerve fibre groups from conduction velocity histograms and picking up single fibre Ap's by wave form analysis. In this way, it is partly possible to clarify functions of the PNS and the CNS in the normal and pathological stages.

### 5.2. *Experimental diabetes and electrodiagnosis during sural nerve biopsies in neuropathies*

It has been shown in experimental diabetes in rats, induced by streptozotocin or alloxan, that reduced conduction velocities can be observed before morphological changes (45). Similar to figure 13, conduction velocity and diameter spectra could also be constructed for rats. Since the sural nerve also contains efferents (7, cat), it is possible to see reduced peak conduction velocities in different touch afferent and  $\alpha$ -motoneuron classes in rat experimental diabetes (49). Additionally, Ap's which had rather large amplitudes and long durations, and which were conducted slowly, were often observed, indicating the existence of thick axons with a functionally damaged myelin sheath (49), since, on average, fast conducting fibers generate Ap's with large amplitudes and short durations in humans (39, 40) and animals (38).

It should be possible to improve the value of sural nerve biopsies (19) for the diagnosis of neuropathies by first recording extracellular Ap's with 2 pairs of electrodes from a small fascicle. In addition to the nerve fibre diameter distribution histogram one would obtain conduction velocity histograms with certain peak values of touch afferents and  $\alpha$ -motoneurons, because the human sural nerve may also have efferents. Such an extended diagnosis would also give information about the changes in the motor system.

### 5.3. *Sacral nerve root stimulation for the control of the urinary bladder in paraplegia*

The urinary bladder function can be improved in paraplegia and other disorders (11) by stimulating lower sacral ventral roots. Unwanted reflex activity has to be expected in some patients from the ventral root afferents (40). If the dorsal sacral roots are cut to reduce reflex activity from the stimulated bladder, dorsal root efferents (61, Table 1) are also cut. Since there are more efferents in the S4 and S5 dorsal roots than in the S3 one it is probable

that the detrusor, mainly innervated by S3 (S4) (1, 30), is not, or only a little, disturbed, whereas the external urethral sphincter, mainly innervated by S4 (S5) (31), may in some cases be essentially weakened. The effect of bladder stimulation, that is the earlier relaxation of the sphincter than the detrusor during continuous stimulation in such cases, may be partly due to the cut sphincteric motoneurons in the dorsal roots. Intraoperative diagnosis, including the recording of single Ap's, in order to verify the existing innervation of the operated patients, may help to arrange the stimulation electrodes in more optimal way. Cutting dorsal roots should be avoided if possible, not only because of the cutting of dorsal root motoneurons, but also because other afferents may take over denervated synapses at the motoneuron somas and interneurons by sprouting (32, 35), so that unwanted reflex changes may appear as time goes on.

#### 5.4. Urogenital malformation and prostate cancer

The method of restoring bladder and bowel continence, in children with urogenital malformation and other patients with the musculus gracilis (29), could probably improved with the knowledge of nerve anastomosis, discussed in the second paper (41). In the case of prostate cancer removals, patients often lose sexual potency and bladder functions. In some cases these functions could be saved, if important nerve branches close to the prostate capsula carrying those functions, could be identified and saved during an operation.

#### Acknowledgements

I am grateful to the following persons for help, advice and the offer of research possibilities: K. Borchert, J. Cervós-Navarro, A. Gräfe, H. Gräfe, D. Hof, G. Lang, B. Richter, H. Schmidt and R. Warzok.

#### References

1. ALLOUSSI, Sch., LOEW, F., MAST, G.J. and WOLF, D.: Die selektive Nervenblockade zur Behandlung der Detrusorhyperreflexie der Harnblase. *Urologe*, A23: 39-45, 1984.
2. ARBUTHNOTT, E.R., BOYD, I.A. and KALU, K.U.: Ultrastructural dimensions of myelinated peripheral nerve fibre in the cat and their relation to conduction velocity. *J. Physiol.*, 308: 125-157, 1980.
3. BAUMANN, H., JÄGGI, M., SOLAND, F., HOWALD, H. and SCHAUB, M.C.: Exercise training induces transitions of myosin subunits within histochemically typed human muscle fibres. *Plügers Arch.*, 409: 349-360, 1987.
4. BEHSE, F. and BUCHTHAL, F.: Normal sensory conduction in the nerves of the leg in man. *J. Neurol. Neurosurg. Psychiat.*, 34: 404-414, 1971.
5. BOHM, E.: Sacral rhizopathies and sacral root syndroms (SII-SV). *Acta chirurgica Scandinavia (suppl.)*, 216: 5-48, 1956.
6. BORS, E. and COMARR, A.E.: *Neurological Urology*. Karger, Basel, 1971.
7. BOYD, I.A. and DAVEY, M.R.: *Composition of peripheral nerves*. Livingston, Edinburgh, 1968.
8. BOYD, I.A. and WARD, J.: Motor control of nuclear bag and nuclear chain intrafusal fibres in isolated living muscle spindles from the cat. *J. Physiol.*, 244: 83-112, 1975.
9. BOYD, I.A., GLADDEN, M.H., MCWILLIAM, P.N. and WARD, J.: Control of dynamic and static nuclear bag fibres and nuclear chain fibres by gamma and beta axons in isolated cat muscle spindles. *J. Physiol.*, 265: 133-162, 1977.
10. BOYD, I.A. and KALU, K.U.: Scaling factor relating conduction velocity and diameter for myelinated afferent nerve fibres in the cat hindlimb. *J. Physiol.*, 289: 277-297, 1979.
11. BRINDLEY, G.S., POLKEY, C.E., RUSHTON, D.N. and CARDOZO, L.: Sacral anterior root stimulation for bladder control in paraplegia: the first 50 cases. *J. Neurol. Neurosurg. Psychiat.*, 49: 1104-1114, 1986.
12. BROWN, A.G. and IGGO, A.: A quantitative study of cutaneous receptors and afferent fibres in the cat and rabbit. *J. Physiol.*, 193: 707-733, 1967.
13. BUCHTHAL, F. and ROSENFALCK, A.: Evoked potentials and conduction velocity in human sensory nerves. *Brain Research*, 3: 1-122, 1966.
14. BUCHTHAL, F. and SCHMALBRUCH, H.: Motor unit of mammalian muscle. *Physiological Reviews*, 60: 91-142, 1980.
15. BURKE, R.E., LEVINE, D.N., TSAIRIS, P. and ZAJAK III, F.E.: Physiological types and histochemical profiles in motor units of the cat gastrocnemius. *J. Physiol.*, 234: 723-748, 1973.
16. CORDA, M., VON EULER, C. and LENNERSTRAND, G.: Reflex and cerebellar influences on  $\alpha$  and on rhythmic and tonic  $\gamma$  activity in the intercostal muscle. *J. Physiol.*, 184: 898-923, 1966.

17. DESMEDT, J.E. and CHERON, G.: Spinal far-field components of human somatosensory evoked potentials to posterior tibial nerve stimulated with oesophageal derivations and non-cephalic reference recording. *Electroenceph. Clin. Neurophysiol.*, 56: 635-651, 1983.
18. DUTHIE, H.L. and GAIRNS, F.W.: Sensory nerve endings and sensation in the anal region of man. *Brit. J. Surg.*, 47: 585, 1960.
19. ERLANGER, J. and GASSER, H.S.: Electrical signs of nervous activity. Philadelphia, University of Pennsylvania Press, 1937.
20. FLESHMAN, J.W., MUNSON, J.B., SYPERT, G.W. and FRIEDMAN, W.A.: Rheobase, input resistance, and motor unit type in medial gastrocnemius motoneurons in the cat. *J. Neurophysiol.*, 41: 1326-1338, 1981.
21. GASSER, H.S. and GRUNDFEST, H.: Axon diameter in relation to the spike dimension and the conduction velocity in mammalian A fibres. *Am. J. Physiol.*, 127: 393-414, 1939.
22. GUSTAFSON, B. and PINTER, M.J.: Relations among passive properties of lumbar  $\alpha$ -motoneurons of the cat. *J. Physiol.*, 356: 401-431, 1984.
23. HUNT, C.C.: Relation of function to diameter in afferent fibres of muscle nerve. *J. gen. Physiol.*, 38: 117-131, 1954.
24. HUNT, C.C. and MCINTYRE, A.K.: An analysis of fibre diameter and receptor characteristics of myelinated cutaneous afferent fibres in the cat. *J. Physiol.*, 153: 99-112, 1960.
25. HURSH, J.B.: Conduction velocity and diameter of nerve fibres. *Am. J. Physiol.*, 127: 131-139, 1939.
26. IGGO, A.: Tension receptors in the stomach and the urinary bladder. *J. Physiol.*, 128: 593-607, 1955.
27. KERNELL, D. and ZWAAGSTRA, B.: Input resistance, axonal conduction velocity and cell size among hind-limb motoneurons of the cat. *Brain Research*, 204: 311-326, 1981.
28. KERNELL, D.: Organisation and properties of spinal motoneurons and motor units. *Progress in Brain Research*, 64: 21-30, 1986.
29. KIRCHNER, H., KIENE, S. and FESTGE, O.-A.: Manometrische Untersuchungen zur Kontinenzleistung bei Patienten nach Grazilisplastik. *Zbl. Chirurgie*, 110: 1258-1262, 1985.
30. KUHN, R.A.: A note on identification of the motor supply to the detrusor. *J. Neurosurg.*, 6: 320-323, 1949.
31. LAWSON, J.: Pelvic anatomy. I Pelvic floor muscles. *Annals of the Royal College of Surgeons of England*, 54: 244-252, 1974.
32. LIU, C.N. and CHAMBERS, W.W.: Intraspinal sprouting of dorsal root axons. *Arch. Neurol. Psychiatr.*, 79: 46-61, 1958.
33. LLOYD, D.P.C.: Neuron patterns controlling transmission of ipsilateral hind limb reflexes in cat. *J. Neurophysiol.*, 6: 293-315, 1943.
34. MILEDI, R., PARKER, I. and SCHALOW, G.: Calcium transients in normal and denervated slow muscle fibres of the frog. *J. Physiol.*, 318: 196-206, 1981.
35. MARRAY, M.: Axonal sprouting in response to dorsal rhizotomy. In: Kao, C.C., Bunge, R.P. and Reier, P.J. (eds.), *Spinal cord reconstruction*. Raven Press, New York, 445-453, 1983.
36. NEWSON DAVIS, J.: The response to stretch of human intercostal muscle spindles studied in vitro. *J. Physiol.*, 249: 561-579, 1975.
37. PAINTAL, A.S.: Effect of temperature on conduction in single vagal and saphenus myelinated nerve fibres of the cat. *J. Physiol.*, 180: 20-49, 1965.
38. PAINTAL, A.S.: The influence of diameter of medullated nerve fibres of cats on the rising and falling phases of the spike and its recovery. *J. Physiol.*, 184: 791-811, 1966.
39. SCHALOW, G.: Single unit potential amplitude in relation to the conduction velocity in frog and human. *Zent. bl. Neurochir.*, 48: 109-113, 1987.
40. SCHALOW, G.: Efferent and afferent fibres in human sacral ventral nerve roots: basic research and clinical implications. *Electromyogr. Clin. Neurophysiol.*, 29: 33-53, 1989.
41. SCHALOW, G.: Oscillatory firing of single human sphincteric  $\alpha_2$  and  $\alpha_3$ -motoneurons reflexly activated for the continence of urinary bladder and rectum. — Restoration of bladder function in paraplegia. *Electromyogr. Clin. Neurophysiol.*, 31: 323-355.
42. SCHALOW, G.: Coactivity of secondary spindle afferents and  $\alpha_2$ ,  $\alpha_3$ ,  $\gamma_1$  and  $\gamma_2$ -motoneurons innervating anal and urinary bladder sphincters in human. *Electromyogr. Clin. Neurophysiol.*, 31: 223-241.
43. SCHMIDT, H. and STEFANI, E.: Re-innervation of twitch and slow muscle fibres of the frog after crushing the motor nerves. *J. Physiol.*, 258: 99-123, 1976.
44. SCHMIDT, H. and STEFANI, E.: Action potential in slow muscle fibres of the frog during regeneration of motor nerves. *J. Physiol.*, 270: 507-517, 1977.
45. SHARMA, A.K. and THOMAS, P.K.: Peripheral nerve structure and function in experimental diabetes. *Journal of the neurological Sciences*, 23: 1-15, 1974.
46. STEIN, R.B.: Peripheral control of movement. *Physiological Reviews*, 54: 215-243, 1974.
47. TODD, J.K.: Afferent impulses in the pudendal nerves of the cat. *Q. Jl. exp. Physiol.*, 49: 258-267, 1964.
48. VALLBO, A.B., HAGBARTH, K.-E., TOREBJÖRK, H.E. and WALLIN, B.G.: Somatosensory, proprioceptive, and sympathetic activity in human peripheral nerves. *Physiological Reviews*, 59: 919-957, 1979.
49. WATTIG, B., SCHALOW, G. and WARZOK, R.: In preparation.
50. WAXMAN, S.G.: Variations in axonal morphology and their functional significance. In: Waxman, S.G. (ed.), *Physiology and Pathophysiology of axons*. Raven Press, New York, 169-190, 1978.
51. WILLIS, W.D. and COGGESHALL, R.E.: *Sensory mechanisms of the spinal cord*. John Wiley & Sons, New York, Table 2.1, 1978.
52. WINTER, D.L.: Receptor characteristics and conduction velocities in bladder afferents. *J. psychiat. Res.*, 8: 225-235, 1971.

53. JOHANSSON, R.S.: Tactile sensibility in the human hand: receptive field characteristics of mechanoreceptive units in the glabrous skin area. *J. Physiol.*, 281: 101-123, 1978.
54. KNIBESTÖL, M.: Stimulus-response functions of rapidly adapting mechanoreceptors in the human glabrous skin area. *J. Physiol.*, 232: 427-452, 1973.
55. KNIBESTÖL, M.: Stimulus-response functions of slowly adapting mechanoreceptors in the human glabrous skin area. *J. Physiol.*, 245: 63-80, 1975.
56. SCHUSTER, M.M.: Motor action of rectum and anal sphincters in continence and defecation. In: Heidel, W. (ed.), *Handbook of Physiology*, Section 6, Alimentary canal, Vol. IV, Mobility. American Physiolog. Society, Washington D.C., 2121-2146, 1968.
57. SCHALOW, G.: *Elektrophysiologische und morphologische Untersuchungen zur Differenzierung der Tonusfasern des Frosches*, Doktorarbeit, Universität des Saarlandes, 1983.
58. PIERROT-DESEILLIGNY, E. and MORIN, C.: Evidence for supraspinal influences on Renshaw inhibition during motor activity in man. In: Desmedt, J.E. (ed.), *Progress in clinical neurophysiology*, Vol. 8, Spinal and supraspinal mechanisms of voluntary motor control and locomotion. Karger, Basel, 142-169, 1980.
59. BARKER, D., EMONET-DÉNAND, F., LAPORTE, Y. and STANCEY, M.J.: Identification of the intrafusal endings of skeletofusimotor axons in the cat. *Brain Research*, 185: 227-237, 1980.
60. PROCHAZKA, A. and HULLIGER, M.: Muscle afferent function and its significance for motor control mechanisms during voluntary movements in cat, monkey, and man. In: Desmedt, J.E. (ed.), *Advances in neurology*, Vol. 39, Motor control mechanisms in health and disease. Raven Press, New York, 93-132, 1983.
61. SCHALOW, G. and LANG, G.: Electrodiagnosis of human dorsal sacral nerve roots by recording afferent and efferent extracellular action potentials. *Neurosurg. Rev.*, 12: 223-232, 1989.
62. DENNY-BROWN, D. and ROBERTSON, E.G.: The state of the bladder and its sphincters in complete transverse lesions of the spinal cord and cauda equina. *Brain*, 56: 397-463, 1933.

Address reprint requests to:

G. Schalow, Dr. med., Dr. rer. nat., Dipl. Ing.  
Weddigenweg 49  
D-1000 Berlin 45  
West Germany

MAXI-B<sup>®</sup> 5000

MAXI-B<sup>®</sup> 5000



SA **labaz-sanofi** NV  
Avenue De Béjar laan 1  
1120 Bruxelles - Brussel